Transmission System Restoration Strategies

in Real Time

by

Chong Wang

A Dissertation Presented in Partial Fulfillment
of the Requirements for the Degree
Doctor of Philosophy

Approved November 2010 by the
Graduate Supervisory Committee:

Vijay Vittal, Chair
Daniel Tylavsky
Gerald Heydt
Richard Farmer

ARIZONA STATE UNIVERSITY

December 2010

ABSTRACT

After a power system blackout, system restoration is the most important task for the operators. Most power systems rely on an off-line restoration plan and the experience of operators to select scenarios for the black start path. Using an off-line designed restoration plan based on past experience may not be the most reliable approach under changing network configurations and loading levels. Hence, an objective restoration path selection procedure, including the option to check constraints, may be more responsive in providing directed guidance to the operators to identify the optimal transmission path to deliver power to other power plants or to pick up load as needed.

After the system is subjected to a blackout, parallel restoration is an efficient way to speed up the restoration process. For a large scale power system, this system sectionalizing problem is quite complicated when considering black-start constraints, generation/load balance constraints and voltage constraints. This dissertation presents an ordered binary decision diagram (OBDD) –based system sectionalizing method, by which the splitting points can be quickly found. The simulation results on the IEEE 39 and 118-bus system show that the method can successfully split the system into subsystems satisfying black-start constraints, generation/load balance constraints and voltage constraints.

A power transfer distribution factor (PTDF)-based approach will be described in this dissertation to check constraints while restoring the system. Two types of restoration performance indices are utilized considering all possible restoration paths, which are then ranked according to their expected performance

characteristics as reflected by the restoration performance index. PTDFs and weighting factors are used to determine the ordered list of restoration paths, which can enable the load to be picked up by lightly loaded lines or relieve stress on heavily loaded lines.

A transmission path agent can then be formulated by performing the automatic path selection under different system operating conditions. The proposed restoration strategy is tested on the IEEE-39 bus system and on the Western region of the Entergy system. The testing results reveal that the proposed strategy can be used in real time.

DEDICATION

To my beloved fiancée, Weijie Hu, my father Dusheng Wang and mother Jing Du, for their love and support through all these years.

ACKNOWLEDGEMENTS

I have been amazingly fortunate to have an advisor who would listen and give advice, encourage and guide me during the whole work with this dissertation. I would like to thank my advisor, Dr. Vijay Vittal. Without his support and advice I can never imagine that I could finish this dissertation. It is an honor for me to be his student.

I am also grateful to the committee members of my Ph.D. dissertation, Prof. Richard Farmer, Dr. Gerald Heydt, Dr. Jennie Si and Dr. Tylavsky. Their valuable suggestions contributed significantly to this work.

In addition, I am indebted to Dr. Kai Sun. Based on his research I completed the OBDD-based system sectionalizing method for power system parallel restoration. The discussions with him enlightened me so much in my research.

Furthermore, I would like to thank PSerc and Entergy for their financial and technical support.

Finally, I would like to thank all my friends in our power group. I have enjoyed every moment that we worked together. I want especially to thank Di Shi, Xianjun Zhang, Sangsu Noh and Guangyue Xu. I will always remember the days with you.

TABLE OF CONTENTS

CHAPTER Page

LIST OF TABLES

Table Page

LIST OF FIGURES

Figure Page

Figure Page

Figure Page

NOMENCLATURE

AC	Alternate current
A_G	Adjacency matrix of an *N*–node network *G(V, E, W)*
$A_{G_{ij}}$	The element of A_G in *i*-th row and *j*-th column
A_G^*	Obtained from logic operation of adjacency matrix
$A_{G_{ij}}^*$	The element of A_G^* in *i*-th row and *j*-th column
$A_{G_{i^*}}^*$	The *i*-th row of A_G^*
b_{ij}	Boolean variable, element of adjacency matrix A_G
BP	Balanced partition
BSC	Black-start constraint
d	The allowable power balance error tolerance
DC	Direct current
$f(x_1, \ldots, x_n)$	Boolean function of variables $x_1, \ldots, x_n$
E	The branch set of network *G(V, E, W)*
E_C	The branch set that splits *G* into two connected sub-graphs $G_1(V_1, E_1, W_1)$ and $G_2(V_2, E_2, W_2)$
GR	Generation rescheduling
G(V, E, W)	Connected and node-weighted graph
I	Identity matrix (1 on the diagonal and 0 elsewhere)
I_A	Subset of I_G, with $I_A=\{i \mid v_i \in V_A^G\}$
I_G	The serial numbers of all generator nodes in the network
I_{ij}	Current from bus *i* to bus *j*

I_k	Current injection on bus *k*
I_{kr}	Real part of I_k
I_{ki}	Imaginary part of I_k
I_S	Subset of I_G, with $I_S=\{j \mid v_j \in V_S^G\}$
L	The longest path in *G(V, E, W)* in terms of the number of branches
LS	Load shedding
NB	The number of buses in the current system
NERC	North American Electric Reliability Corporation
NL	The number of lines in the current system
NP	Non-deterministic polynomial time
NPc	NP-complete
OBDD	Ordered binary decision diagram
O(n)	The order of the time complexity of checking the satisfiability of a Boolean function $f(x_1, \ldots, x_n)$
PBC	Power balance constraint
P_G^i	The injected real generator power at bus *i*
P_L^i	The real load power at bus *i*
RPI	Restoration performance index
S_G^i	The injected complex generator power at bus *i*
SI	System islanding
$\overline{S_{ij}}$	The complex power flow in the line from bus *i* to bus *j*
S_k	Injected complex power on bus *k* (i.e., MVAs)
S_L^i	The complex load power at bus *i*

$\overline{\Delta S_p}$	The power flow change on line number p
ΔS_q	The power injection change on bus number q
TOC	Transmission operations center
TSI	Transient stability index
TSR	Transmission system reconfiguration
UPFC	Unified power flow controller
V	The node set of $G(V, E, W)$
VSC	Voltage stability constraint
V_A^G	Subset of generator group
V_S^G	Subset of generator group
W	The weight set of $G(V, E, W)$
x_i	The i-th Boolean variable
Z_{bus}	Bus impedance matrix referenced to the swing bus
Z_{bus}^{new}	Bus impedance matrix referenced to the swing bus after system topology changes
Z_{bus}^{old}	Bus impedance matrix referenced to the swing bus before system topology changes
Z_{im}	The element in the i-th row, m-th colomn of impedence matrix
Z_{imr}	Real part of Z_{im}
Z_{imi}	Imaginary part of Z_{im}
Z_{jm}	The element in the j-th row, m-th colomn of impedence matrix
Z_{jmr}	Real part of Z_{jm}

Z_{jmi}	Imaginary part of Z_{jm}
η	Transient stability index
$\rho_{ij,k}$	Power transfer distribution factor relating the loading in the line from bus *i* to bus *j* with respect to injected complex power on bus *k*
$\rho_{lm,n}^{add\_ij}$	Power transfer distribution factor relating the loading in the line from bus *l* to bus *m* with respect to injected complex power on bus *n* with addition of line from bus *i* to bus *j*
$\Delta\rho^{add\_line}$	Power transfer distribution factor change matrix with addition of a candidate line
δ_{max}	Maximum generator relative angle difference
ω_k	Weighting factor of branch *k*
$\otimes$	The logic "AND" operation
$\oplus$	The logic "OR" operation
$\overline{\oplus}$	The logic "EXCLUSIVE-OR" operation

CHAPTER 1

INTRODUCTION

Power system restoration involves a broad diversity of tasks. Among the numerous complicated factors restoration of the system to normal operation as quickly as possible is the primary restoration objective. In general, restoration is a decision making process in which a set of actions are carried out by the system operators to mitigate the outage.

1.1 Power System Operation States

When the bulk transmission system is subjected to large disturbances there is the possibility of a system wide blackout due to cascading outages. A suitable preventive or corrective control scheme is needed to protect the system from these disturbances and outages. In order to facilitate the investigation of power system security and design of appropriate control strategies, power systems can be conceptually classified into five operational states: normal, alert, emergency, in extremis, and restorative [1], which are shown in Fig. 1.1[2].

Normal State: No system component is being overloaded. All the system variables are in the normal range and the system operates in a secure state and is able to withstand a contingency without violating any constraints.

Alert state: The system enters the alert state when the system condition is degraded. In this state, all the system variables are still within the acceptable range and no constraints have been violated. However, the system components may be overload when an *N*-1 contingency occurs and leads the system into an emergency state. The system may also directly transit from the alert state to the in

extremis state if the disturbance is severe enough.

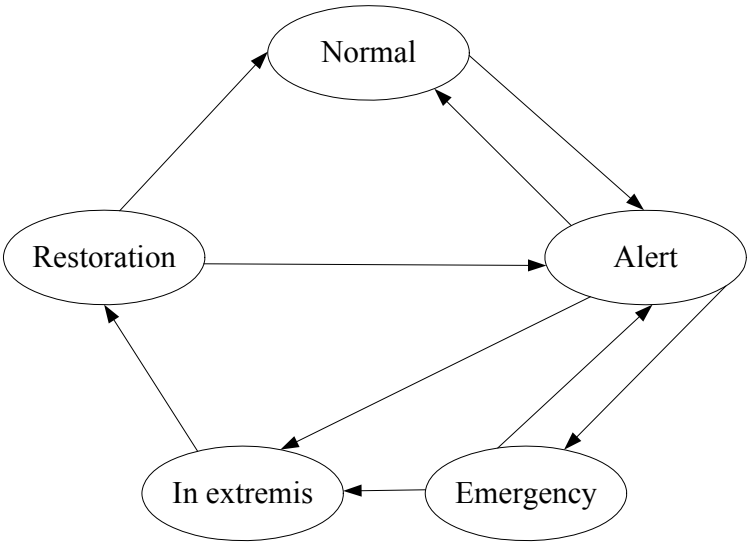

Fig. 1.1 Power system operating states [2]

Emergency state: When the system is in the alert state, a sufficiently large contingency event may bring the system to the emergency state, where system voltages at many buses go below the normal range and the one or more system components may experience overloading. In this state, the system may be restored back to the alert state by initiating corrective control strategies such as transmission system reconfiguration (TSR), generation rescheduling (GR), and load shedding (LS).

In Extremis: The system enters the in extremis state if the appropriate corrective controls are not applied or are ineffective when the system is in the emergency state. Corrective control strategies in this state include load shedding (LS) and system islanding (SI). These controls are intended to prevent total system blackout and preserve as much of the system as possible.

Restorative State: This state depicts a condition where control strategies are being deployed to reconnect all system components and to restore system load. Depending on the system condition, the system may transfer to the alert state, or directly transit back to the normal state.

The North American Electric Reliability Corporation (NERC) planning standards [3] define two components of reliability, 1) adequacy of supply and 2) transmission security:

Adequacy is the ability of electric systems to supply the aggregate electrical demand and energy requirements of customers at all times, taking into account scheduled and reasonably-expected unscheduled outage of system elements.

Security is the ability of electric systems to withstand sudden disturbances such as electrical short circuits or unanticipated loss of system elements.

Corrective control strategies provide solutions to the security problem in situations such as circuit overload, voltage problems, and transient problems.

1.2 Power System Restoration

During the past few decades, considerable effort has been directed toward studying the topics of preventive and corrective control. But restoration plans differ in specificity based on the characteristics of different power systems. Generally, the restoration process can be divided into three discrete stages: preparation, system restoration, and load restoration.

The goals and objectives of restoration can be mainly grouped into the following three categories:

- To restore all loads safely

- Minimize duration of outages
- Minimize unserved loads.

The restoration strategy is also affected by different types of outages:

- Partial system
- Full system with outside assistance
- Full system without outside assistance.

With regard to these considerations, there are several issues that should be considered during system restoration, among which a few can be listed as follows:

(1) Load and generation balance

It is necessary to maintain the system frequency by determining the rate of response of the prime movers, from which the rate of load pick-up can then be determined. A change of frequency may also occur if: 1) there exists a load-generation mismatch, 2) if the rate at which a generator can be loaded is limited. By bringing the units with fast rates of response and proper reactive absorbing capabilities online, early in the restoration, the process can be shortened by a significant time.

(2) Reactive power balance

During the early stages of the restoration, system voltages should also be maintained within an acceptable range, usually a little bit lower than the normal level. Because low load levels at the receiving end of transmission may raise the system voltages due to Ferranti effects. There are several ways to solve this problem: 1) energizing fewer high voltage lines, 2) operating generators at minimum voltage levels, 3) deactivating shunt capacitors/activating shunt reactors, or 4)

picking up load with a lagging power factor. In the literature [3], several problems related to reactive power balance have been described, such as sustained over-voltages and under-voltages, generator under-excitation, and switched shunt capacitors/reactors.

(3) Black-start capability or remote cranking power capability

According to the NERC criterion, all power system utilities should have black-start capability arrangements to enable a restart in the unexpected event that all or part of the system is out of service. Black-start generators should be included in each subsystem of the power system, so that they can start restoration individually and then gradually be reconnected in order to restore system integrity.

1.3 Problem Statement

System restoration following a power system blackout is one of the most important tasks of the operators in the control center. However, few computer tools have been developed and implemented for the on-line operational environment. Actually, most power systems rely on off-line restoration plans, which are developed for selected scenarios of contingencies. Since the actual outages are hard to predict in the planning stage, the restoration plan can only serve as a guide. System operators need the near real-time system information to make decisions with changing system conditions during system restoration.

In this research effort, the objective is to develop a computational tool that can be used to provide guidance to the system operators in the operational environment so that system restoration can adapt to the changing system conditions. Two aspects of the restoration strategy will be discussed in the following chapters:

1. An approach to split the system into suitable islands or subsystems that would facilitate parallel restoration.
2. An approach to select restoration paths automatically and to check limiting constraints as the bulk transmission system is being restored.

1.4 Literature Review

The history of power system blackouts and restoration dates back to the early 1940s. In the early stages of evolution of the electric grid, the bulk system voltage ratings were low and the size of the system in comparison to the size of the current interconnected systems was quite small. System blackouts were mainly due to natural calamities, such as floods and storms. The literature contains few publications during this period. The early restoration activities were presented in [3], and some actual restoration cases was described in [4], [5]. In the late 20th century, expert system technology and knowledge-based methods were utilized in power system restoration. Among these publications, some expert system applications are found which are real-time expert systems for fault analysis and restoration [6]. A more efficient system restoration method is required for most modern electric power utilities.

Most electric utilities have developed system restoration plans to meet the needs of their own particular systems. These plans contain general guidelines for the system operators. But using a restoration plan which is designed based on the past experience and off line analysis may not be the most reliable approach as it is difficult to predict changing network configurations and loading levels as restoration proceeds.

There are several papers describing system restoration guidelines and policies [7], [8]. Among all these strategies, the restoration plan can be subdivided according to how the cranking power is supplied into the power stations: (i) cranking power is from black-start generators in the outaged area, (ii) receiving cranking power from adjacent power system. In both strategies, parallel restoration is considered to be an efficient strategy and the details of this approach will be given in next chapter.

There are some papers concerning systematic or algorithmic approaches to system restoration. These include: (i) re-energizing the power system at extremely low voltages [9], (ii) algorithmic restoration control system [10]. The idea of method (i) is to re-energize the power system at extremely low voltages and then connect the unloaded power network. The system voltages will increase with addition of unloaded lines into the power network. In method (ii), it is assumed that an adjacent power network is operating normally and ready to supply cranking power to initiate restoration in the outaged area. Reference [11] provides a systematic procedure to restore a power network with overload and abnormal voltage checking.

1.5 Dissertation Organization

This dissertation is organized as follows. Chapter 2 presents an overview of the OBDD-based system sectionalizing strategy. Chapter 3 presents the PTDF-based restoration path selection algorithm. Chapter 4 presents the steps to recreate the system conditions that existed on June 15, 2005, that led to the storm-related outages in the Western region of the Entergy System. Several illustrative exam-

ples of the application of the proposed technique for restoring systems are also presented in Chapter 4. Conclusions drawn from the application are presented in Chapter 5.

CHAPTER 2

OBDD-BASED SYSTEM SECTIONALIZING STRATEGY

Power system restoration involves a broad diversity of tasks. Among the numerous complicated factors restoration of the system to normal operation as quickly as possible is the primary restoration objective. A centralized black-start capability could accomplish the cranking task to restore the entire system with a sequential restoration strategy. However, the time required to restore a large system by this method may be significantly longer. Hence, a parallel restoration method is commonly used by utilities in system restoration plans [12]. In the case of widespread blackouts, it is almost always advantageous to sectionalize the affected area into several subsystems to utilize parallel restoration of subsystems, and thus reduce restoration duration. Liu et al. suggest generic restoration actions (GRAs) [13]. These are termed: preparation, system restoration and load restoration. The first stage is to partition a system into subsystems and send cranking power to non-black-start generators. The second and third stages are reintegration of the bulk power network and minimize the impact of the outage by gradually picking up load.

The resynchronization of the subsystems is quite time consuming due to communication complexities and the lack of measurement data during the early stages of restoration. To bring the entire critical load to service and restore significant load as quickly as possible before the synchronization of subsystems, a methodology of sectionalizing strategy is required. This chapter focuses on the optimized strategy for the first stage and introduces a three-step OBDD-based search

procedure, which can assist the system operator, by providing efficient sectionalizing strategies during restoration. The results can be provided in near real-time and are capable of handling unexpected system changes during restoration. A common parallel restoration sequence includes:

1. Sectionalizing of power system into subsystems
2. Restoration of each subsystem
3. Synchronization of subsystems

The determination of the parallel restoration sequence to be used in restoring a specific system is highly dependent on the system conditions. An inappropriate sectionalizing strategy can cause difficulty in synchronization of subsystems or cause restored load to be tripped again. Several criteria require to be verified before the parallel restoration determination in order to maintain system security and restoration reliability. These criteria include [12],[14]:

1. Each subsystem must have at least one black-start generator;
2. Each subsystem should match generation and load to maintain system frequency within prescribed limits;
3. Each subsystem should have adequate voltage control capabilities to maintain a suitable voltage profile;
4. Each subsystem should be monitored at the system control center to ensure its internal security.

In an effort to solve the problem taking into account the first three criteria above, a balanced partition problem (BP Problem) based approach is considered [15].The BP problem consists of determining proper strategies to ensure that the

black-start generator constraint is satisfied, and the generation/load imbalance is limited. The BP Problem has been proven to be *NP-complete* [15], i.e. no polynomial time algorithm can solve it. The search space for solutions exponentially explodes with the growth in the number of transmission lines, whose on/off status is described by an equal number of Boolean variables. Since the BP problem contains a large number of Boolean variables corresponding to the transmission lines in a large power system, it is difficult and time consuming to determine all proper solutions. The ordered binary decision diagram (OBDD) based sectionalizing approach can improve the solution efficiency of complex Boolean equations and has been widely used in the solution of other large partitioning problems [16], [17]. The OBDD-based methods have been previously applied in solving power system islanding strategies [18], [19]. This chapter will focus on checking steady-state stability of the subsystems formed. After sectionalizing strategies are obtained by the proposed three-step method, transient stability can be checked by simulations on critical contingencies or line closing operations [20]. The sectionalizing strategies with all the parallel restoration constraints satisfied are candidates for the system dispatcher to consider in parallel restoration. After the search results are provided by the proposed method, the operator can select the best strategy based on updated system configuration and experience. Without loss of generality, only the case of sectionalizing one network into two subsystems is considered in the following sections. The approach can be extended to the more general case with more subsystems without loss of generality.

2.1 BP Problem in Power System Restoration

Not all generating plants are suitable candidates for black-start units. During the parallel restoration process, all the available generators can be divided into two categories:

- Black-start generators – which are capable of providing cranking power to a de-energized power system.
- Non-black-start generators – which are incapable of providing power to a de-energized power system. The state space representation of an *n*th order dynamic system without any input is considered

After the entire system is sectionalized into subsystems, each subsystem must have at least one black-start generator to provide power to non-black-start generators to carry out subsystem restoration. This constraint is denoted as a black-start constraint (*BSC*).

Each subsystem in the developed parallel restoration scheme should have the ability to match generation and load to a prescribed tolerance to maintain system frequency. Moreover, if the available generation level is close to the predicted load level inside each subsystem, a larger portion of the subsystem can be restored to facilitate the synchronization of subsystems. This constraint is denoted as the power balance constraint (*PBC*).

When the subsystems are being synchronized, some open lines on the boundary of subsystems may cause system voltage problems. In the network related aspects, the critical lines that maintain system voltage stability should not be

included on the sectionalizing boundary in the final sectionalizing strategy. This constraint is denoted as the voltage stability constraint (*VSC*).

The following BP problem consists of finding the sectionalizing strategies that satisfy *BSC* and *PBC* constraints identified above during parallel restoration.

If there are *NL* branches in the power system, there are 2^{NL} possible branch state combinations to check *BSC* and *PBC* constraints. Hence, the BP problem of a large-scale power system is quite time consuming and complicated because a combinatorial explosion of its strategy space is unavoidable. Moreover, it is necessary to guarantee both correctness and speed in determining the final sectionalizing strategy to speed up restoration. The *satisfiability* of the Boolean expression of the sectionalizing strategy is developed and solved in Section 2.3 below. After the BP problem is solved, all the transmission lines should be evaluated to make sure no voltage violation occurs during subsystem synchronization.

The BP problem can be analytically stated as follows, given an undirected, connected and node-weighted graph $G(V, E, W)$, two subsets V_{GA}, V_{GS} of V and a positive constant d, search for a subset E_C to split G into two connected subgraphs $G_1(V_1, E_1, W_1)$ and $G_2(V_2, E_2, W_2)$ such that $V_{GA} \subset V_1$, $V_{GS} \subset V_2$ (*BSC*) and the following constraint (*PBC*) are satisfied:

$$\left| \sum_{v_i \in V_1} w_i \right| \leq d \,, \qquad \left| \sum_{v_j \in V_2} w_j \right| \leq d \tag{2.1}$$

where $V=\{v_1, ..., v_n\}$ is the node set, d is the allowable power balance error tolerance, E is the branch set. $W=\{w_1, ..., w_n\}$ is the weight set; w_i can be calculated by the following equation:

$$w_i = S_G^i - S_L^i \tag{2.2}$$

where S_G^i is the injected complex generator power and S_L^i is the complex load power at bus i. In this chapter, the restoration paths inside the subsystems are not considered and will be described in Chapter 3. Reactive power imbalance is highly related with energizing sequence. In the actual power network, the unbalanced reactive power can be compensated by local reactive power compensators, and the real power balance and real power flow are more important during restoration. So only the real power balance is considered, and the weight of node i in the power network is defined by the following equation:

$$w_i = P_G^i - P_L^i \tag{2.3}$$

2.2 OBDD Representation

It has been proved that the problem of determining *satisfiability* of Boolean expressions is NP-complete [21]. This check of *satifiability* involves the determination of whether the Boolean expression has value "0" or "1". An OBDD [22] is a directed acyclic graph (DAG) representation of a Boolean expression and is commonly used to determine *satisfiability* of Boolean expressions. The time complexity of checking the *satisfiability* of a Boolean function $f(x_1, ..., x_n)$ is $O(n)$. Once the OBDD of a function is built, its *satisfiability* can be verified in polynomial time. But the choice of variable ordering of $x_1, ..., x_n$ cannot be solved in polynomial time and has significant impact on the size of the OBDD. Once the

variable ordering has been chosen carefully, different kinds of logic operations can be performed efficiently on the OBDD.

Fig. 2.1 below shows an OBDD (the reduction rules have not been applied), representing the function $f(x_1, x_2, x_3, x_4) = x_1 \otimes x_2 \oplus x_3 \otimes x_4$, where the symbol "⊗" represents the "AND" operation, and the symbol "⊕" represents the "OR" operation. In the OBDD, a variable x_i with a "False" value (having value "0") is denoted by a dashed line and the variable x_i with a "True" value (having value "1") is denoted by a solid line. Once all possible values of a variable have been addressed, the OBDD progresses to the next level at which the states of the next variable are addressed. As can be seen from Fig. 2.1, the complete OBDD is complex and can be reduced by applying the following two reduction rules [22], [23]:

1) merging rule—two isomorphic subgraphs should be merged. As shown in Fig. 2.2(a) below, v_1 and v_2 connect to same nodes and they both either have value "0" or "1". Then v_1 and v_2 should be merged into a new node v_3. All nodes that point to v_1 or v_2 are connected to v_3 after reduction.
2) deletion rule—a node whose two branches point to the same node should be deleted. As shown in Fig. 2.2(b) below, both branches of v_4 point to same node irrespective of whether v_4 has value "0" or "1". Then v_4 should be deleted. All nodes pointing to v_4 in the upper level are directly connected to the node that v_4 pointed to before in the lower level.

Applying these rules for reduction, Fig. 2.3 shows the reduced OBDD, from which it is straight forward to get the solution to the *satisfiability* of Boolean expressions problem depicted in Fig. 2.1. There are 3 paths, associated with 7 possible solutions, and the 3 paths are marked using arrows in Fig. 2.3. The result corresponding to each path is shown in Table 2.1. In the table, an "X" associated with a variable means that irrespective of whether the variable x_i is "True" or "False" in that path, the OBDD checking result will remain the same.

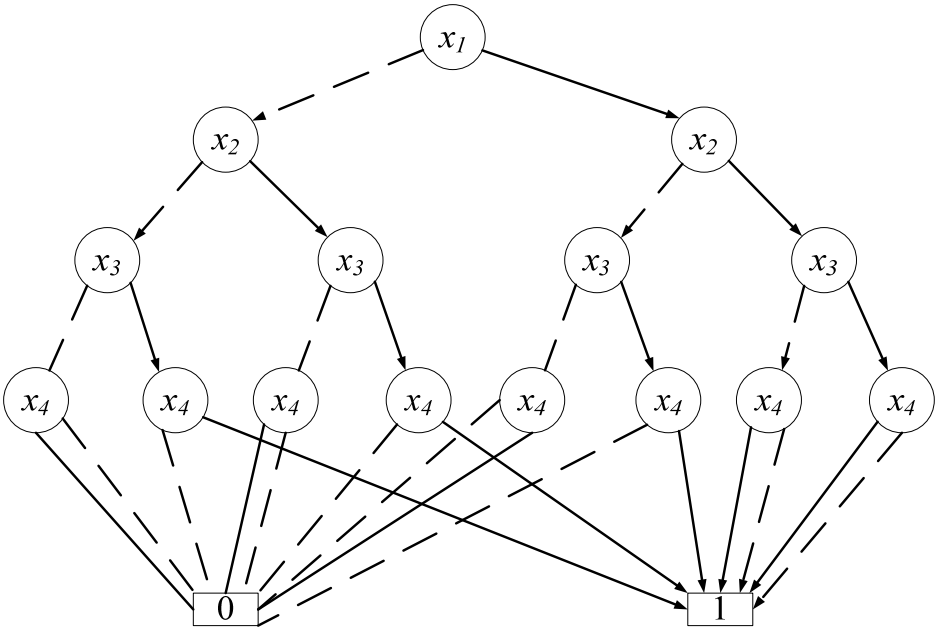

Fig. 2.1 Binary decision diagram representing the function $f(x_1, x_2, x_3, x_4)=\boldsymbol{x_1 \otimes x_2 \oplus x_3 \otimes x_4}$

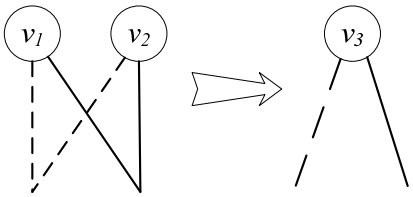

a) Merging rule

b) Deletion rule

Fig. 2.2 OBDD reduction rules

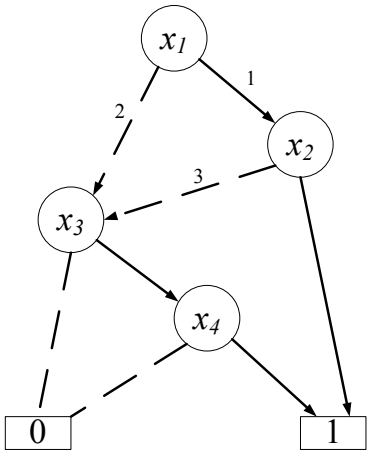

Fig. 2.3 Reduced ordered binary decision diagram representing the function $f(x_1, x_2, x_3, x_4) = \boldsymbol{x_1 \otimes x_2 \oplus x_3 \otimes x_4}$

Table 2.1 Result of OBDD Reduction

Path	x_1	x_2	x_3	x_4
1	1	1	X	X
2	0	X	1	1
3	1	0	1	1

If there are *NL* branches in the power system, there are 2^{NL} possible branch state combinations to check *BSC* and *PBC* constraints. Hence, the BP problem of a large-scale power system is quite time consuming and complicated because a combinatorial explosion of its strategy space is unavoidable. Moreover, it is necessary to guarantee both correctness and speed in determining the final sectionalizing strategy to speed up restoration. The *satisfiability* of the Boolean expression of the sectionalizing strategy is developed and solved in following section.

2.3 OBDD-Based Three-Phase Sectionalizing Strategy

Step-1: Initialize OBDD model based on system information

To create an OBDD for a power system, every branch in the system can be seen as a Boolean variable, with respect to "0" or "1". The branch with number "0" means this branch is open in the final sectionalizing strategy and a branch with number "1" means it is closed in the final sectionalizing strategy. So each root node in the binary decision diagram represents one binary combination of all the branch states, which can be tracked by a bottom-up process.

All branches are then included in the binary decision diagram. For the different system constraints, if one binary combination of all the branch states satisfies all the constraints, then that root node will connect to the terminal node "**1**". If any constraint violation occurs, then that root node will connect to the terminal node "**0**". Using this logic the binary decision diagram can be constructed with any branch order. For a specific power system, there is more than one OBDD with respect to different branch orders, but there is only one set of feasible solutions satisfying a given Boolean expression. For example, a 4-bus system is

shown in Fig. 2.4. It is assumed that both generators are black-start generators. To satisfy the *BSC*, two possible solutions are given: 1) x_1, x_3 are closed and x_2, x_4 are open; 2) x_1, x_3 are open and x_2, x_4 are closed. For this set of possible solutions the binary decision diagram is shown in Fig. 2.5 based on the branch order x_1, x_2 x_3, x_4.

When performing system restoration, operators need near real-time system information in order to make decisions under changing system conditions. Some information is extremely important in parallel restoration. These system conditions include:

- black-start capability
- interconnection assistance
- non-black-start plants status
- status of transmission lines and breakers
- predicted generation and load level inside each subsystem

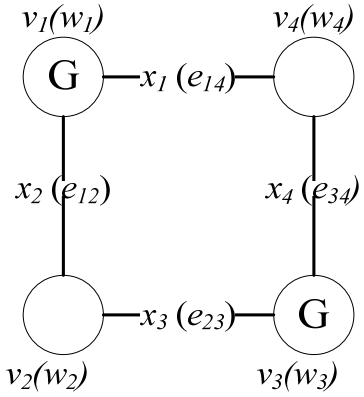

Fig. 2.4 Four-bus power system with two black-start units

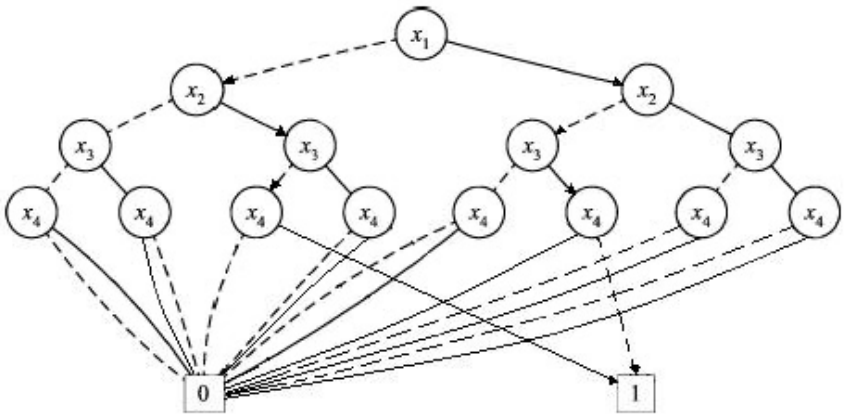

Fig. 2.5 Unreduced binary decision diagram for *BSC* in four-bus power system

After the information is sent to the transmission operations center (TOC), the OBDD parameters are initialized. The black-start unit and critical load are confirmed. The system load is assumed to be about 40% of the total available generator ratings. The binary variables corresponding to the lines with certain open or closed status are assigned values of "0" or "1". System operators can also set the transmission line status (as Boolean value) based on their experience or special concern. This may eliminate some paths of the OBDD representing a feasible operation. The allowable power balance error tolerance d is also chosen by the TOC. Then the binary decision diagram is maximally reduced by applying the two reduction rules in OBDD described in Chapter 2.2.

Step-2: Building OBDD and solving BP problem

Before the Boolean expressions of *BSC* and *PBC* are presented, the concept of the adjacency matrix of an *N*–node network *G(V, E, W)* is introduced. The elements $A_{G_{ij}}$ and $A_{G_{ji}}$ of the adjacency matrix A_G are the same Boolean variable,

denoted by b_{ij}. If there is an edge $e_{ij} \in E$, $A_{G_{ij}} = A_{G_{ji}} = b_{ij} = 1$; otherwise $A_{G_{ij}} = A_{G_{ji}} = 0$. For example, the A_G of the four-bus power system shown in Fig. 2.4 is given by (2.4).

$$A_G = \begin{bmatrix} 0 & b_{12} & 0 & b_{14} \\ b_{12} & 0 & b_{23} & 0 \\ 0 & b_{23} & 0 & b_{34} \\ b_{14} & 0 & b_{34} & 0 \end{bmatrix} \tag{2.4}$$

It is easy to draw the following conclusions from Boolean matrix theory:

$$A_G^* \triangleq I \oplus A_G^1 \oplus A_G^2 \oplus \ldots \oplus A_G^L \tag{2.5}$$

where L is the longest path in *G(V, E, W)*. The path between two arbitrary nodes in the network is the shortest connection in terms of the number of branches. I is identity matrix (1 on the diagonal and 0 elsewhere) which has the same dimension as A_G, and A_G^i is the matrix A_G raised to the i-th power. The symbol "⊕" here represents the "OR" operation on each element of the matrices. Then A_G^* can determine the connection of any arbitrary pair of nodes inside the network. If $A_{G_{ij}}^* = 1$, there must exist a connection path between bus i and bus j.

For example, considering the four-bus power system, L=3 and all the paths from v_1 to v_4 in Fig. 2.4 can be obtained by (2.6).

$$A_{G_{14}}^* = b_{14} \oplus b_{12} \otimes b_{23} \otimes b_{34} \tag{2.6}$$

where b_{14} and $b_{12} \otimes b_{23} \otimes b_{34}$ correspond with paths e_{14} and $e_{12}e_{23}e_{34}$. If the system is sectionalized into two subsystems by opening branch e_{12} and e_{34}, $A_{G_{14}}^* =$

b_{14} =1 by setting b_{12}=b_{34}=0. This represents that bus 1 and bus 4 are connected in the above sectionalizing strategy.

Then the Boolean expression of *BSC* and *PBC* can be built from A_G^*. For the convenience of expression, two sets of generator groups are defined as V_A^G and V_S^G. There is at least one black-start generator in each group. Three sets of serial numbers of the nodes in the network are defined:

$$I_A = \{i \mid v_i \in V_A^G\},\ I_S = \{j \mid v_j \in V_S^G\}$$
$$\text{and } I_G = I_A \cup I_S \tag{2.7}$$

I_G contains the serial numbers of all generator nodes. Select any two arbitrary elements $i_A \in I_A$and $i_S \in I_S$. Then, *BSC* can be expressed as

$$BSC = \prod_{i \in I_A}^{\otimes} A^*_{G\,i,i_A} \otimes \prod_{j \in I_S}^{\otimes} A^*_{G\,j,i_S} \otimes \prod_{k \notin I_G}^{\otimes} \left(A^*_{G\,k,i_A} \overline{\oplus} A^*_{G\,k,i_S} \right) \tag{2.8}$$

where "$\overline{\oplus}$" represents the "EXCLUSIVE-OR" operation. The first two product terms guarantee that all the generators inside each subsystem are connected to each other. The third product term guarantees that each load bus connects to only one black-start generator. Obviously *BSC* is a Boolean function of all b_{ij}s.

Then the *PBC* can be expressed as

$$PBC = \prod_{i=1\ldots N}^{\otimes} \langle \left| A^*_{G\,i^*} \times W \right| < d \rangle \tag{2.9}$$

where $A^*_{G\,i^*}$ is the i-th row of A^*_G and $W = \left[w_{1,} \ldots, w_n\right]^T$ is the real power weight vector of N nodes, which has been introduced in Chapter 2.1. $A^*_{G\,i^*} \times W$ is the real power balance error in the subsystem that contains node number i in the network. Therefore, the product guarantees that the real power balance in each subsystem is smaller than the power balance error tolerance d.

To find an estimate of d, a reduced model of a reheat unit for frequency decline analysis [24], [25] is used. According to the North East Power Coordinating Council (NPCC) standard, the automatic under-frequency load shedding (UFLS) should be deployed immediately if system frequency drops to 57 Hz [26].

Typical system data is used to compute the minimum power balance error that can drive the system to the frequency of 57 Hz for each subsystem restored in parallel. This gives the power balance error tolerance. For a typical reheat turbine model neglecting all smaller time constants, the speed deviation can be expressed as

$$\Delta\omega = \left(\frac{R\Omega_n^2}{DR + K_m}\right)\left(\frac{(1 + T_R s)P_d}{s^2 + 2\Omega_n^2\lambda s + \Omega_n^2}\right) \tag{2.10}$$

where,

$$\Omega_n^2 = \frac{DR + K_m}{2HRT_R} \tag{2.11}$$

$$\lambda = \left(\frac{2HR + (DR + K_m f_H)T_R}{2(DR + K_m)}\right)\Omega_n \tag{2.12}$$

Here K_m is a mechanical power gain factor. A typical value of 0.95 is used.

H inertia constant in seconds, typically 4.0 s;

f_H high-pressure power fraction, typically 0.3;

D damping factor, typically 1.0;

T_R reheat time constant, seconds, typically 8.0 s;

R fraction of the reheat turbine, typically 0.559;

P_d power balance error, in per unit.

P_{sys} real power in entire system

P_{subsys} real power in subsystem

Usually P_d is in the form of a step function. The time domain solution for the speed deviation can be directly obtained from (2.10) as follows

$$P_d = P_{step}u(t) \tag{2.13}$$

$$\Delta\omega = \left(\frac{RP_{step}}{DR + K_m}\right)\left(1 + ae^{-\lambda w_n t}\, sin(\omega_r t + \phi)\right) \tag{2.14}$$

where,

$$a = \sqrt{\frac{1 - 2T_R\lambda\omega_n + T_R^2\omega_n^2}{1 - \lambda^2}} \tag{2.15}$$

$$\omega_r = \omega_n\sqrt{1 - \lambda^2} \tag{2.16}$$

$$\phi = \phi_1 - \phi_2 \tag{2.17}$$

$$\phi_1 = \tan^{-1}\left(\frac{\omega_r T_R}{1 - \lambda\omega_n T_R}\right) \tag{2.18}$$

$$\phi_2 = \tan^{-1}\left(\frac{\sqrt{1 - \lambda^2}}{-\lambda}\right) \tag{2.19}$$

Using this reduced model and normalizing, the lowest system average frequency for this disturbance is obtained as 57 Hz when P_d = 0.11P_{sys}. So, 0.11P_{subsys} is chosen as the power balance error limit in each subsystem. A lower *d* value is selected to improve system frequency response during load restoration procedure based on system conditions. The system frequency deviation for different values of power balance error is shown in Fig. 2.6.

Variable orderings of b_{ij} are selected based on the node weights. The branch with the *larger sum* of the two ending nodes weights of that branch has a higher order. This ordering is more efficient than the random orderings. Then the OBDDs of *BSC* and *PBC* can be developed and simplified using the OBDD software packages. Finally, the OBDD of the *BP* problem is obtained by applying operation "AND" on *BSC* and *PBC* expressions.

$$BP = BSC \otimes PBC \tag{2.20}$$

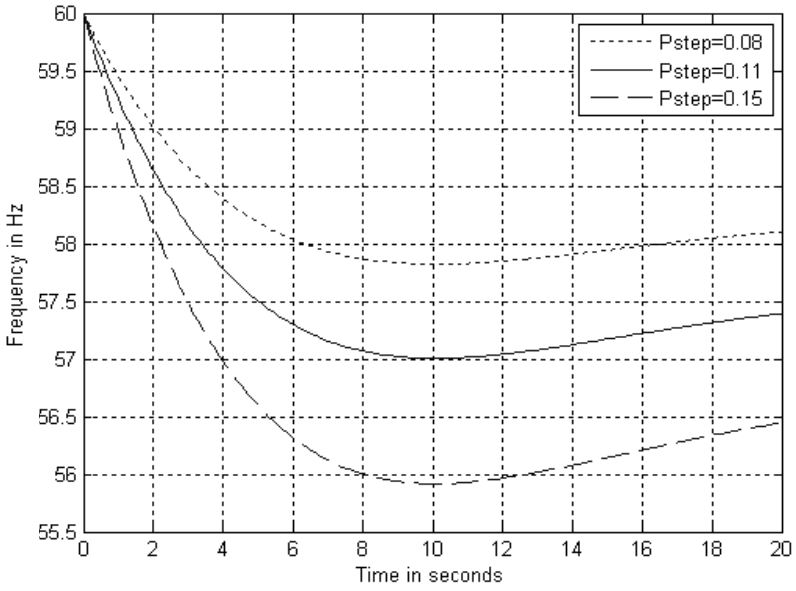

Fig. 2.6 Frequency response to different power balance error value

Step-3: Identifying voltage critical tie-lines

During the synchronization of the subsystems, the open boundary tie-lines can be considered as outaged lines before they are closed. To identify critical lines that cannot lie at the sectionalizing boundary, *N*-1 voltage stability analysis is conducted for all line outages in the system. The most severe outages are selected using the contingency screening method available in VSAT [27].

The contingency screening feature in VSAT is designed to identify the critical contingencies. The screening feature of critical line contingencies classifies all the possible contingencies based on their voltage stability margin. The voltage stability margin of each contingency is defined as the difference between the pre-contingency transfer at the initial operating point and the last point where the post-contingency solution exists [27].

In this phase, all the sectionalizing strategies from *Step-2* are evaluated based on their voltage stability performance. The candidate strategy with critical lines on the boundary will be eliminated. Moreover, the voltage stability margin of each contingency inside the subsystems can be obtained as needed.

Fig. 2.7 shows the flow chart of the proposed three-step OBDD-based search procedure.

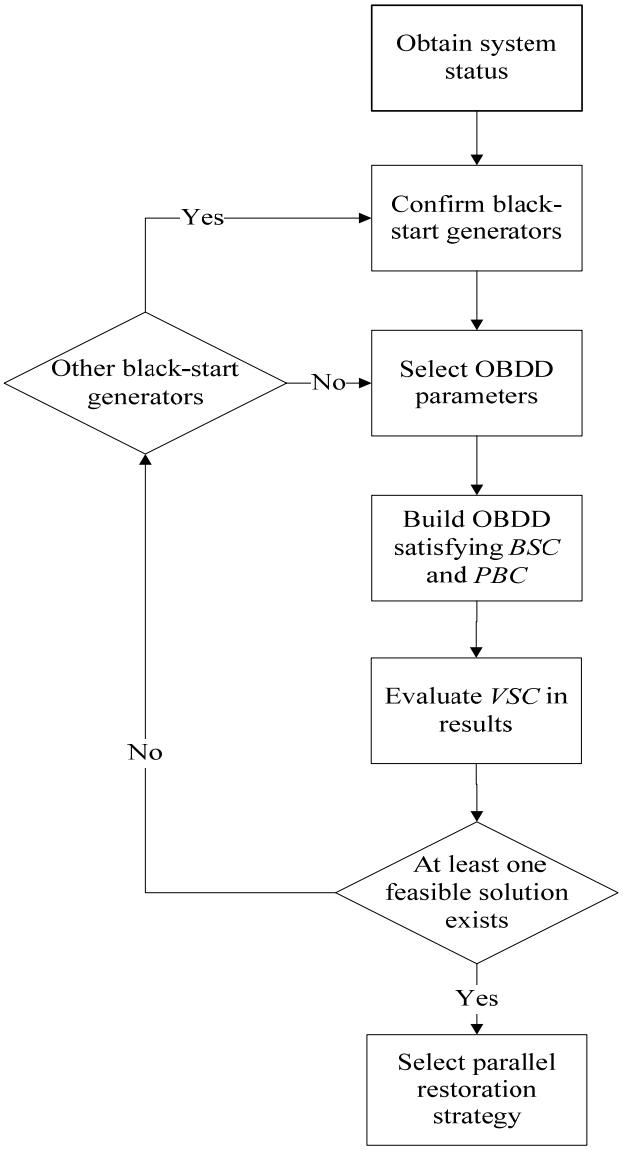

Fig. 2.7 Parallel restoration strategies searching method flow chart

2.4 Simulation Results

A. Simulation Results for the IEEE 39-bus Network

Several assumptions are made before the BP problem is solved using OBDD algorithm. There are 10 generator buses in the system, two of them are

assumed to be the black-start units. They are bus 30 and bus 36, which are shown in the first row of Table 2.2. To find all the possible solution among $2^{34}\approx1.718\times10^{10}$ possible choices, it is assumed that bus 30 will send cranking power to buses with serial numbers $I_A=\{30, 31, 32, 37 \text{ and } 39\}$; bus 36 will send cranking power to buses with serial numbers $I_S=\{36, 33, 34, 35 \text{ and } 38\}$. The total generation in the entire system is 6192.9 MW and the total load is 6150.1 MW. The generation/load balance error in each subsystem is selected as d=90 MW.

The ordering of Boolean variables is set as follows (using the criterion based on the sum of the ending nodes weights):

$$b_{3,4} < b_{7,8} < b_{15,16} < b_{16,24} < b_{16,21} < b_{23,24} < b_{8,9} < b_{5,8} < b_{4,14} < b_{4,5} < b_{28,29} < b_{3,18} < b_{26,29} < b_{26,27} < b_{25,26} < b_{26,28} < b_{16,19} < b_{16,17} < b_{2,3} < b_{14,15} < b_{17,27} < b_{21,22} < b_{22,23} < b_{6,7} < b_{2,25} < b_{17,18} < b_{9,39} < b_{1,39} < b_{13,14} < b_{10,13} < b_{10,11} < b_{6,11} < b_{5,6} < b_{1,2}$$

With the black-start constraint and generation/load constraint checking, the total search time on a 34-branch system is less than 4.77 seconds. Only two paths, associated with two sectionalizing strategies without any constraint violations are found. The results are shown in Table 2.3 and Fig. 2.8.

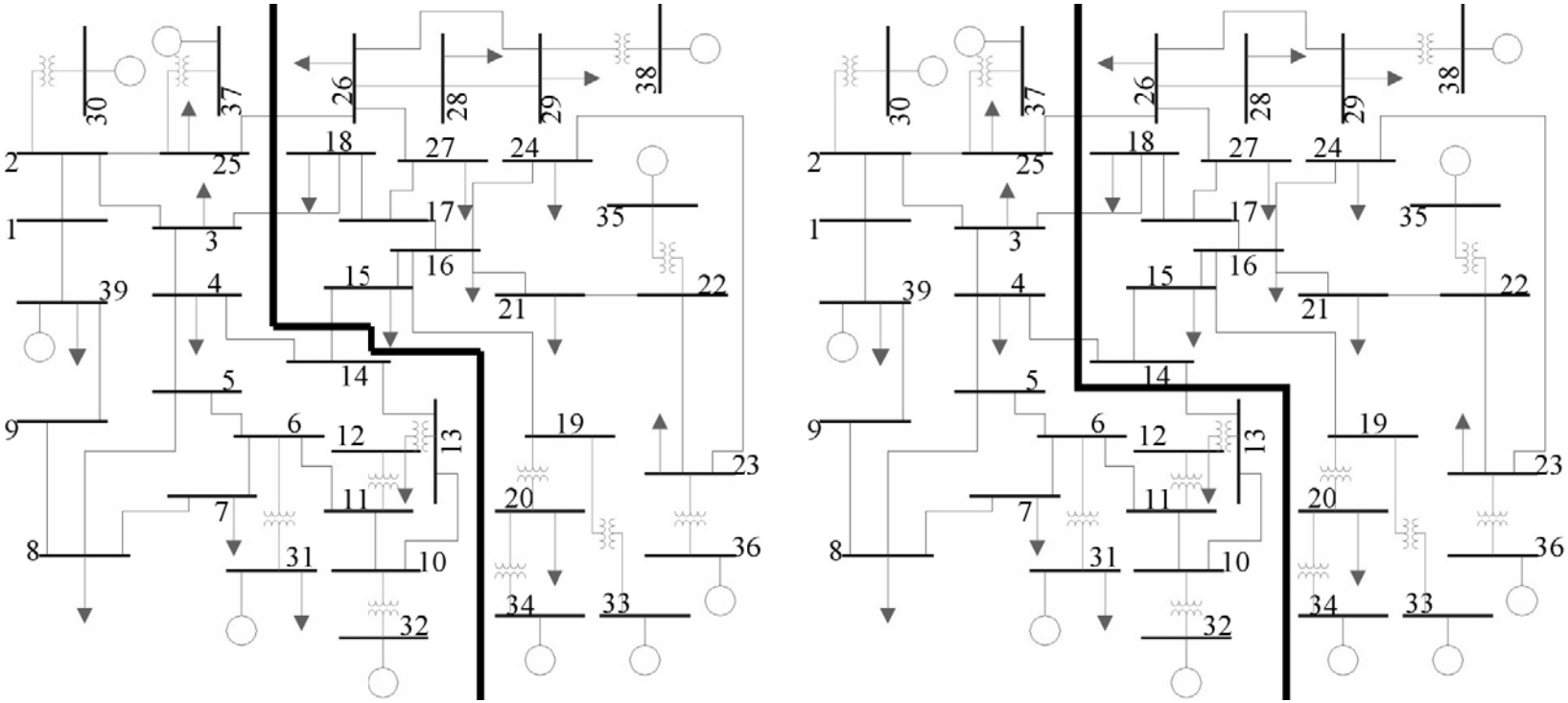

a) Sectionalizing strategy No.1 b) Sectionalizing strategy No.2

Fig. 2.8 Sectionalizing strategy on IEEE 39-bus system

Table 2.2 Generator Data of IEEE 39-Bus System

Bus No. (I_A)	P_G (MW)	Bus No. (I_S)	P_G (MW)
30	250.00	**36**	560.00
31	572.87	33	632.00
32	650.00	34	508.00
37	540.00	35	650.00
39	1000.00	38	830.00

Table 2.3 Sectionalizing Searching Results of IEEE 39-Bus System

Number	Cut-set lines between two sub-systems	Generation and load mismatch (MW)
1	3-18, 14-15, 25-26	89.4, -46.6
2	3-18, 4-14, 13-14, 25-26	89.4, -46.6

B. Simulation Results for the IEEE 118-Bus Network

In this section, the standard IEEE 118-bus data is used to verify the proposed method. There are 186 branches in the network. To accelerate the search, a network simplification method introduced in [19] can be used. In this paper the network simplification is not considered and the original network is used. The generation/load mismatch limit is chosen as d =150 MW. The real-power generator data is shown in Table 2.4. Several assumptions are made before the BP problem is solved using the OBDD algorithm. Bus 31 and bus 87 are assumed as black-start generators and the cranking groups are given in Table 2.5. The selection of the cranking groups is based on the generators synchronization groups in contingency analysis when their synchronization is lost [18]. The generation level

is reduced to about 40% of generation ratings with the entire critical load in service.

There are 211 possible sectionalizing strategies. The results for the critical contingency screening based on voltage performance are shown in Table 2.6 based on the maximum power transfer level. After eliminating the candidate strategies which contain these voltage stability vulnerable lines, there are 137 strategies that satisfy *BSC*, *PBC* and *VSC*. Fig. 2.9 shows one possible system sectionalizing strategy. Six lines are open in the sectionalizing strategy, they are

$$\{e_{15,33}, e_{19,34}, e_{30,38}, e_{69,70}, e_{70,74}, e_{70,75}\}$$

Table 2.4 Generator Data of IEEE 118-Bus System

Bus No.	P_G (MW)	Bus No.	P_G (MW)	Bus No.	P_G (MW)
10	180.00	54	19.20	87	1.60
12	34.00	59	62.00	89	242.80
25	88.00	61	64.00	100	100.80
26	125.60	65	156.40	103	16.00
31	2.80	66	156.80	111	14.40
46	7.60	69	206.40		
49	41.60	80	190.80		

Table 2.5 Generator Cranking Groups of IEEE 118-Bus System

Group No.	Node Serial Numbers	Total real power generation (MW)
1	**31**, 10, 12, 25, 26	431
2	**87**, 46, 49, 54, 59, 61, 65, 66, 69, 80, 89, 100, 103, 111	1274

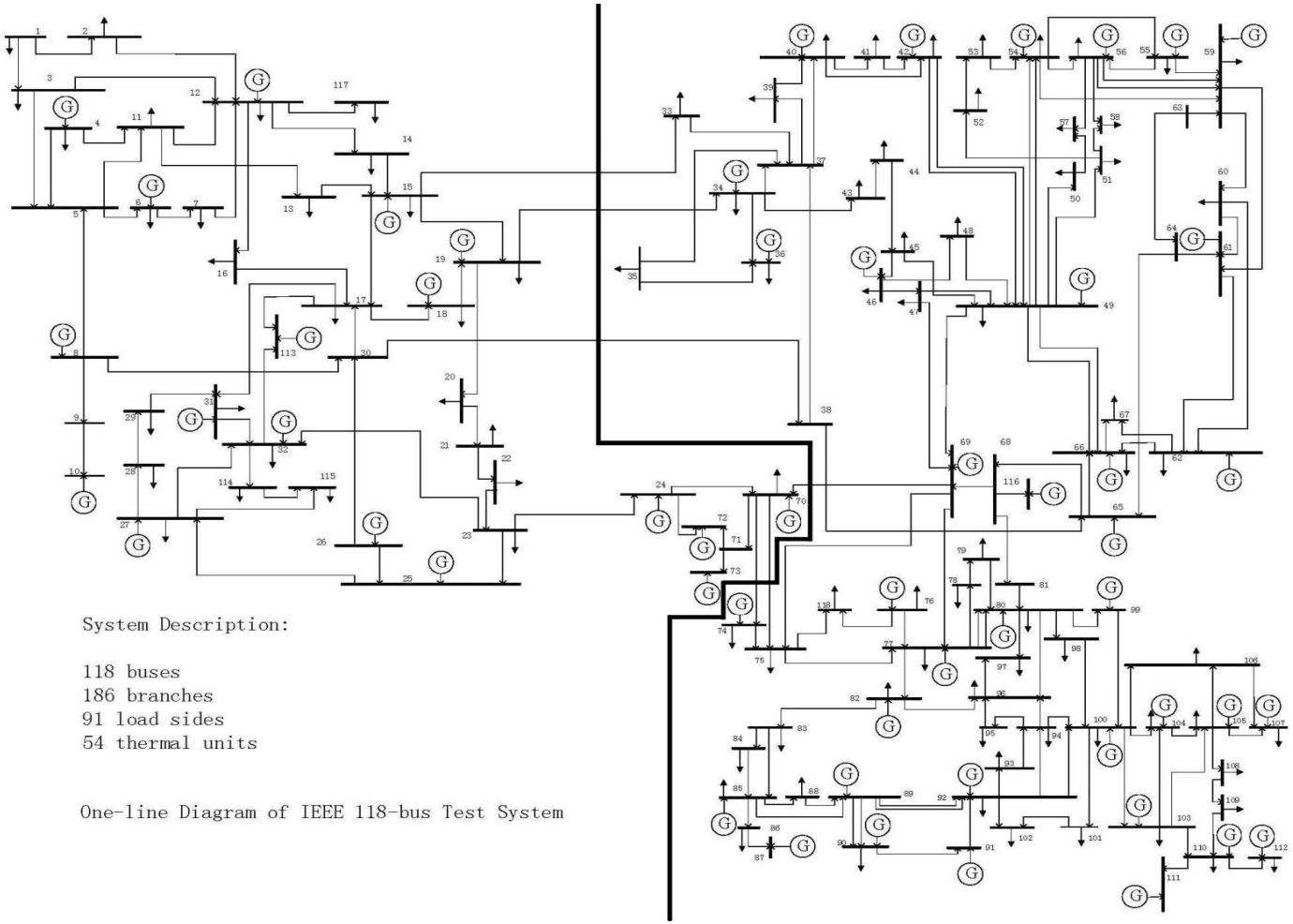

Fig. 2.9 Sectionalizing strategy on IEEE 118-bus system

Table 2.6 Voltage Stability Screening on IEEE 118-Bus System

Rank	Type	From Bus Number	To Bus Number	Zone
1	Line	8	9	1
2	Line	9	10	1
3	Line	38	65	1
4	Line	8	5	1
5	Line	38	37	1

The BuDDy package (v2.0) [28], which supports all standard OBDD operations and especially many highly efficient OBDD vector operations, is selected to develop a program in C++ language on a PC (Core2 6700-2.66G CPU and 2.0GB DDRAM). The package has evolved from a simple introduction to OBDDs to all the standard OBDD operations.

With the black-start constraint and generation/load constraint checking, the total search time on a 186-branch system is less than 3 minutes.

These results reveal that the checking module found two solutions for the BP problem. In the actual case, once it is determined that parallel restoration is feasible for the system, the operators only need to consider the two selected candidate strategies instead of all 2^{186} strategies. This is a very big saving in time. The operators' final decision will be made with consideration of the current state of system and availability of alternative generators and lines. If none of the sectionalizing strategies are suitable for the current system status, the operator can change the generation cranking group or relieve power balance error tolerance for further searching.

It should be noted that the generators' cranking group can be different. To maximize the generation capability, all the non-black-start generators are considered available during the restoration. The problem of optimizing generation capability during the restoration is complex and involves a large number of combinatorial choices [29]. A number of constraints have to be verified before initiating the cranking process. The constraints mainly include voltage and frequency transient, voltage drop and protective relay actions [30]. Hence, the black-start and non-black-start generators start-up sequence should be adjusted depending on real time generator status. Moreover, from the network topology it is observed that arbitrary generator groups cannot guarantee that there is a sectionalizing strategy. In the actual case, the operators have to evaluate the generator groups considering these constraints and cranking sequence. If the system does not have enough generation capability in each subsystem, the load level in the subsystems should be reduced. Before all the generating units are restored or the subsystems are synchronized, operators should maintain the generation/load balance in the subsystems.

2.5 Impact of the Sectionalizing Strategy on the Parallel Restoration

This section presents an efficient approach to search for system sectionalizing strategies using the OBDD-based technology. The proposed method decomposes the splitting search process into three parts: 1) determination of branch status and ordering in OBDD, 2) finding the boundary of the subsystems under the black-start constraint and constraint of minimizing the generation/load imbalance error, 3) evaluation of system voltage stability during parallel restoration.

The proposed approach will sectionalize the system into suitable islands or subsystems that would facilitate parallel restoration. Then a sequential restoration would accomplish the restoration in each subsystem. After the subsystems are restored, the tie-lines could be energized to synchronize subsystems. The method was tested on the IEEE 118-bus test networks. The results indicate that method is effective during the early stages of the restoration as they provide guidance to the operators on how parallel restoration could be performed.

The method focuses on the first stage of the restoration. It gives the system operators direct guidance with respect to sectionalizing strategy and generator cranking groups. The results can be provided in real time after system condition change. This three-step method may not be the final sectionalizing strategy. And there is no need to stick to the rigid boundary of the subsystems. The OBDD variable values can be updated with the unpredicted system condition changes or specified by operators. This chapter provides a search method that augments the operators' capabilities. The constraints can also be updated and checked with operator choices after OBDD searching.

CHAPTER 3

PTDF-BASED AUTOMATIC RESTORATION PATH SELECTION

This chapter examines the restoration path selection for the blacked-out transmission systems based on efficient checking of the thermal, transient stability and voltage constraints on the transmission system after the affected area has sufficient power supply/generation available. The algorithm determines the restoration path to restore the area, however, the lines identified for restoration may not to be energized simultaneously, and each transmission switching operation should be checked and verified carefully for safety constraints prior to energizing the lines.

In an effort to reduce the time duration and cost related to service interruption, and to check some of these constraints, several analytical tools have been proposed, such as: expert systems [31]-[32] and heuristic approaches [33]. These methods integrate knowledge from the operators and computational algorithms such as power flow and transient stability software to optimize the restoration process and to verify that constraints are not violated. In this dissertation, a computational tool that can be used to provide guidance to the dispatchers in the operational environment so that system restoration can adapt to the changing system conditions is proposed.

3.1 PTDF-Based Restoration Path Selection

To determine the correct sequence for energizing the lines, the concept of PTDF [34] and weighting factors are used. This idea was originally developed in contingency analysis and evaluated for the removal of branches or the loss of ge-

nerators at specific nodes. In this dissertation the novelty of the approach is to plan restoration by calculating the PTDFs for candidate lines to be closed. Even though the concept of PTDF is well established, the use of this idea in system restoration is unique and has not been attempted before.

To use the linear approximation, the calculation of PTDFs involves the derivatives of complex numbers. For the derivatives to be valid, the equations must obey the Cauchy-Riemann requirement. The Cauchy-Riemann requirements are briefly described as follows.

Let $f(x+jy)=u+jv$ be the complex equation in question, f is holomorphic if and only if u and v are continuously differentiable and their partial derivatives satisfy the Cauchy-Riemann equations, which are:

$$\frac{\partial u}{\partial x}=\frac{\partial v}{\partial y}, \qquad \frac{\partial u}{\partial y}=-\frac{\partial v}{\partial x} \tag{3.1}$$

If a line is a radial line between buses i and j, the change in power flow on the radial line due to a complex power injection at another bus k can be evaluated [35]. The PTDF relating the loading in the line from bus i to bus j with respect to the injected complex bus power S_k on bus k, is denoted as $\rho_{ij,k}$.

$$\rho_{ij,k}=\frac{\partial S_{ij}}{\partial S_k}=\frac{\partial I_{ij}^{*}V_j}{\partial I_k^{*}V_k} \tag{3.2}$$

To prove that (3.2) obeys the Cauchy-Riemann requirement, the approximation of near unity bus voltage magnitude is applied to (3.2).

$$\rho_{ij,k}=\frac{\partial I_{ij}^{*}V_j}{\partial I_k^{*}V_k}=\frac{\partial I_{ij}^{*}}{\partial I_k^{*}} \tag{3.3}$$

$$I_{ij}^{*} = \left(\frac{V_i - V_j}{z_{ij}}\right)^{*} = \left(\frac{1}{z_{ij}}\right)^{*} \sum_{m=1}^{NB} (Z_{im} - Z_{jm})^{*} I_m^{*} \tag{3.4}$$

It is assumed that $I_k = I_{kr} + jI_{ki}$, $Z_{im} = Z_{imr} + jZ_{imi}$ and $Z_{jm} = Z_{jmr} + jZ_{jmi}$.

$$I_{ij}^{*} = \left(\frac{1}{z_{ij}}\right)^{*} \sum_{m=1}^{NB} \left(Z_{im} - Z_{jm}\right)^{*} I_m^{*}$$

$$= \left(\frac{1}{z_{ij}}\right)^{*} \sum_{m=1}^{NB} \left\{\left[\left(Z_{imr} - Z_{jmr}\right) + j\left(Z_{jmi} - Z_{imi}\right)\right]\left(I_{mr} - jI_{mi}\right)\right\} \tag{3.5}$$

From (3.3),

$$\frac{\partial u}{\partial x} = \left(\frac{1}{z_{ij}}\right)^{*} \frac{\partial\left[\left(Z_{imr} - Z_{jmr}\right)I_{kr} + \left(Z_{jmi} - Z_{imi}\right)I_{ki}\right]}{\partial I_{kr}} = \left(\frac{1}{z_{ij}}\right)^{*} \left(Z_{imr} - Z_{jmr}\right),$$

$$\frac{\partial v}{\partial y} = \left(\frac{1}{z_{ij}}\right)^{*} \frac{\partial\left[\left(Z_{jmi} - Z_{imi}\right)I_{kr} - \left(Z_{imr} - Z_{jmr}\right)I_{ki}\right]}{\partial(-I_{ki})} = \left(\frac{1}{z_{ij}}\right)^{*} \left(Z_{imr} - Z_{jmr}\right),$$

$$\frac{\partial u}{\partial y} = \left(\frac{1}{z_{ij}}\right)^{*} \frac{\partial\left[\left(Z_{imr} - Z_{jmr}\right)I_{kr} + \left(Z_{jmi} - Z_{imi}\right)I_{ki}\right]}{\partial(-I_{ki})} = -\left(\frac{1}{z_{ij}}\right)^{*} \left(Z_{jmi} - Z_{imi}\right),$$

$$\frac{\partial v}{\partial x} = \left(\frac{1}{z_{ij}}\right)^{*} \frac{\partial\left[\left(Z_{jmi} - Z_{imi}\right)I_{kr} - \left(Z_{imr} - Z_{jmr}\right)I_{ki}\right]}{\partial I_{kr}} = \left(\frac{1}{z_{ij}}\right)^{*} \left(Z_{jmi} - Z_{imi}\right)$$

(3.6)

The Z elements in the equations above are obtained from the bus impedance matrix. V_i is the bus voltage at bus i. z_{ij} is the primitive impedance of the line connecting bus i to bus j. From (3.6), it is obvious that PTDF equation satisfies the Cauchy-Riemann equations.

3.2 Radial Lines Restoration Performance Index

In the approach developed, restoration performance indices (RPIs) will be calculated for ranking two types of branch closures.

During the transmission restoration process, all the newly added lines can be divided into two categories:

1. Radial lines – which will create a branch between an existing node and a new node.
2. Loop closure lines – which will complete paths between two existing nodes.

The restoration time period, in which the transmission system is restored, usually takes 3 to 4 hours [19]. In order to speed up system restoration in the absence of system constraint violations, it is assumed that the radial lines will be candidates to be restored first, rather than loop closure lines.

If the distribution factors are arranged in a rectangular array, the power transfer distribution factor matrix can be formed as

$$\begin{bmatrix} \overline{\Delta S_1} \\ \overline{\Delta S_2} \\ . \\ . \\ \overline{\Delta S_{NL}} \end{bmatrix}_{NL} = \begin{bmatrix} \rho_{11} & \rho_{12} & . & . & \rho_{1\,NB} \\ \rho_{21} & \rho_{22} & . & . & \rho_{2\,NB} \\ . & . & . & & . \\ . & . & & . & . \\ \rho_{NL\,1} & \rho_{NL\,2} & . & . & \rho_{NLNB} \end{bmatrix}_{NL\,*\,NB} \begin{bmatrix} \Delta S_1 \\ \Delta S_2 \\ . \\ . \\ \Delta S_{NB} \end{bmatrix}_{NB} \tag{3.7}$$

where,

NL is the number of lines in the current system

NB is the number of buses in the current system

$\overline{\Delta S_p}$ is the power flow change on line number *p*

ΔS_q is the power injection change on bus number *q*

After a new radial line with load at the end of the line is restored in the system, the power flow on the lines that have already been restored will change.

The capability of different restored transmission lines to sustain this power flow change will also be different. For example, a lightly loaded line will be able to withstand a higher power flow increase than a moderately loaded line when a radial line with load is restored in the system. The change in power flow with each possible line addition can be estimated using the PTDF calculation with respect to the existing system topology.

If all the restored lines are not close to their thermal limit, the existing power flow expressed as a percentage of the thermal limit on each restored line will be used as a weighting factor ω on the change in power flow (obtained from PTDFs) to evaluate each candidate radial line path restoration. A restoration performance index (RPI) is then evaluated for each candidate radial line considered. The RPI is the sum of the products of the weighting factor and power flow change in each existing transmission line. For each candidate radial line, its RPI is the sum of the products of the weighting factor and power flow change in each existing transmission line. Then, the candidate radial line with the lowest value of its RPI vector element is restored first. This index is referred to as a Type 1 RPI:

$$RPI_1 = \sum_{p=1}^{NL} \overline{\Delta S_p} \times \omega_p \tag{3.8}$$

3.3 Loop Closure Lines Restoration Performance Index

If a line with primitive impedance z_{ij} is a loop closure between buses i and j, a new intermediate matrix denoted as Z^{temp} is considered:

Tree collapse is essential to the cutset determination algorithm and guarantees that generators being identified as belonging to the same slowly coherent

group are located in the same island. The idea of using tree collapse in islanding was first introduced in [18]; however, in this dissertation the tree collapse algorithm developed is both effective and efficient in handling large power systems.

$$Z^{temp} = \begin{bmatrix} Z_{bus}^{old} & col_i Z_{bus}^{old} - col_j Z_{bus}^{old} \\ row_i Z_{bus}^{old} - row_j Z_{bus}^{old} & (Z_{bus}^{old})_{ii} + (Z_{bus}^{old})_{jj} - 2(Z_{bus}^{old})_{ij} + z_{ij} \end{bmatrix} \tag{3.9}$$

To get the new bus impedance matrix, Kron reduction is performed:

$$Z_{bus}^{new} = Z_{bus}^{old} - \Delta_{ij} Z_{loop} \Delta_{ij}^{T} \tag{3.10}$$

$$\Delta_{ij} = (col_i Z_{bus}^{old} - col_j Z_{bus}^{old}) \tag{3.11}$$

$$Z_{loop} = (Z_{bus}^{old})_{ii} + (Z_{bus}^{old})_{jj} - 2(Z_{bus}^{old})_{ij} + z_{ij} \tag{3.12}$$

The Z_{bus}^{old} and Z_{bus}^{new} elements in the equations above are obtained from the bus impedance matrix before and after system topology changes. To calculate the updated PTDF $\rho_{lm,n}^{add\_ij}$ relating the loading in the line from bus *l* to bus *m* with respect to the injected complex bus power S_n on bus *n*, after adding a line from bus *i* to bus *j*, substitute the new bus impedance matrix values obtained from (3.10). The PTDF is then given by:

$$\begin{aligned} \rho_{lm,n}^{add\_ij} &= \frac{[(Z_{bus}^{new})_{ln} - (Z_{bus}^{new})_{mn}]^*}{z_{lm}^*} \\ &= \rho_{lm,n} - \frac{[(Z_{bus}^{old})_{in} - (Z_{bus}^{old})_{jn}]^*}{Z_{loop}^*} \frac{\{[(Z_{bus}^{old})_{il} - (Z_{bus}^{old})_{jl}] - [(Z_{bus}^{old})_{im} - (Z_{bus}^{old})_{jm}]\}^*}{z_{lm}^*} \\ &= \rho_{lm,n} - \frac{[(Z_{bus}^{old})_{in} - (Z_{bus}^{old})_{jn}]^*}{Z_{loop}^*} (\rho_{lm,i} - \rho_{lm,j}) \end{aligned} \tag{3.13}$$

Then, the power transfer distribution factor matrix with the addition of the line from bus i to bus j is obtained as:

$$\begin{bmatrix} \rho_{11}^{add\_ij} & \rho_{12}^{add\_ij} & . & . & . & \rho_{1NB}^{add\_ij} \\ \rho_{21}^{add\_ij} & \rho_{22}^{add\_ij} & . & . & . & \rho_{2NB}^{add\_ij} \\ . & . & & & & . \\ . & & & . & & . \\ . & & & & . & . \\ \rho_{NL1}^{add\_ij} & \rho_{NL2}^{add\_ij} & . & . & . & \rho_{NLNB}^{add\_ij} \end{bmatrix}$$

For each possible loop closure line, a specific matrix $\Delta\rho^{add\_line}$ is evaluated.

$$\Delta\rho^{add\_ij} = \begin{bmatrix} \rho_{11}^{add\_ij} & \rho_{12}^{add\_ij} & . & . & \rho_{1NB}^{add\_ij} \\ \rho_{21}^{add\_ij} & \rho_{22}^{add\_ij} & . & . & \rho_{2NB}^{add\_ij} \\ . & . & . & . & . \\ . & . & . & . & . \\ \rho_{NL1}^{add\_ij} & \rho_{NL2}^{add\_ij} & . & . & \rho_{NLNB}^{add\_ij} \end{bmatrix} - \begin{bmatrix} \rho_{11} & \rho_{12} & . & . & \rho_{1NB} \\ \rho_{21} & \rho_{22} & . & . & \rho_{2NB} \\ . & . & . & . & . \\ . & . & . & . & . \\ \rho_{NL1} & \rho_{NL2} & . & . & \rho_{NLNB} \end{bmatrix} \quad (3.14)$$

This matrix captures the change in each PTDF element due to the addition of the line. If q heavily loaded lines exist in the restored system, restoration of the next radial line can result in limit violations. In such instances, loop closure lines should be first evaluated for restoration in order to relieve the stress on the lines that are almost at their limit. In order to compare the candidate loop closure lines a Type 2 RPI for line i to j is defined:

$$RPI_2 = \sum_{p=1}^{q} \left(\Delta\rho^{add\_ij}\Delta S\right)_p \times \omega_p \quad (3.1)$$

ΔS is the vector of injected complex bus power changes due to the closing of the candidate radial line. Then, the candidate loop closure line with the lowest RPI is restored first, which means that it can relieve the most stress on the

heavily loaded lines.

Fig. 3.1 shows the flow chart of the proposed automatic restoration path selection algorithm. As shown in the flow chart, the algorithm only needs the current system state to determine the next line to be closed, rather than power flow calculations to check the transmission line thermal constraints. All possible transmission lines that can be restored are evaluated. If any line is not available or fails to be closed, operators can consider the next best option from the sorted restoration index list until the blackout area is fully restored.

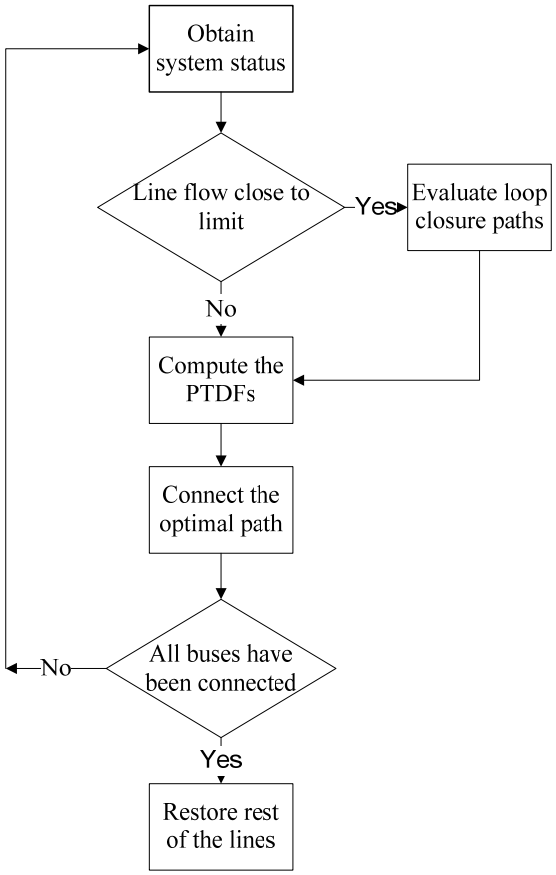

Fig. 3.1 Restoration path selection algorithm flow chart

3.4 *N*-1 Criterion and Area Determination

During the early stages of restoration, a reasonable balance should be maintained between generation and load to avoid frequency deviations [36]. At this time, generation and load in the system are kept at a very low level to maintain system basic operation, and there might be several radial line candidates that have RPI values that are close to each other but could result in the restoration process bringing back to service totally different load areas.

The load areas to be restored should be defined by system operators based on system configuration or load priorities. In the proposed approach if there are more than one load areas, the sequence in which to restore the load areas is determined based on the NERC *N*-1 criterion [37] and system transient security analysis. The area with the largest transient stability margin and least number of insecure contingencies will be restored first.

N-1 contingency analysis is performed on all candidate load areas to be restored using the software package TSAT (DSA^{Tools} [38]). The severity of a contingency can be assessed using the transient stability index (*TSI*). The *TSI* is calculated as follows,

$$TSI = \frac{360 - \delta_{\max}}{360 + \delta_{\max}} \times 100 \qquad -100 < TSI < 100 \tag{3.2}$$

$\delta_{\max}$ is the maximum angle separation of any two generators in the system at the same time in the post-fault response. $TSI > 0$ and $TSI \leq 0$ correspond to stable and unstable conditions respectively. The area with the largest stability margin and least percentage of insecure contingencies should be restored first. This en-

sures that the restored load area would be least susceptible to further degradation due to transient instabilities.

3.5 Line Switching Issues

When energizing lightly loaded transmission lines or underground cables, the excessive VArs generated by the undercompensated high voltage lines can increase voltages to unacceptable high levels which are referred to as sustained power frequency overvoltages. If not controlled, these voltages could cause serious reactive power imbalance resulting in generator self-excitation, transformer overexcitation and harmonic distortions.

Basically, sustained overvoltages can be controlled by absorbing the reactive power generated by the lightly loaded transmission lines. This can be done in several ways [14].

- having sufficient under-excitation capability on the generators
- picking up loads with low power factor
- switching on shunt reactors
- adjusting transformer taps
- operating FACTS controllers, such as SVCs, TCRs and UPFCs.

Due to the fact that adjustments of the control variables are subject to the constraints imposed by plant and system operating conditions, the total effect of these control variables will determine whether the long transmission line can be

energized successfully or not.

3.6 Summary

The suggested approach uses the power transfer distribution factor algorithm and weighting factors to determine the optimal restoration sequence for the transmission system. This path selection procedure is performed mainly by checking system thermal constraints. The stability constraints and voltage constraints are addressed in the following Chapter. The restoration path selection algorithm is intended to assist the system operator during restoration, by providing a restoration index.

CHAPTER 4

SIMULATION RESULTS OF RESTORATION PATH SELECTION

4.1 Overview of Examples and Test Beds

This chapter presents a power transfer distribution factor (PTDF) -based path selection approach for large-scale power systems. Two types of restoration performance indices are utilized considering all possible restoration paths, which are then ranked according to their expected performance characteristics as reflected by the restoration performance index. Test results which are primarily concerned with load restoration in the outaged system are provided based on IEEE 39-bus system and a realistic restoration exercise for the Western region of the Entergy transmission system.

The case studies have been designed with the objective of evaluating the performance of the algorithm. The Western region of the Entergy transmission system is chosen as a realistic case. The entire power supply for the affected area had to be obtained from outside the affected area. IEEE 39-bus system is selected to test the algorithm on a multi-generator outaged system. All simulations were performed in MATLAB 2010 on one PC (Core2 6700-2.66G CPU and 2.0GB DDRAM).

4.2 Test System Data

In June 2005, severe thunderstorms precipitated and forced the interruption of three critical lines in the Western region of the Entergy system. The loss of these lines impacted the ability of the electrical system to serve the Western region load because these lines were tie-lines into the Western region. Within

seconds, the generation and other critical lines in the area tripped, and over several minutes the Western region separated from the rest of the system [39]. The system was restored back to normal within four hours after the disturbance. The Western region of the Entergy network is shown in Fig. 4.1. The proposed power transfer distribution factor (PTDF) -based restoration path selection method is applied to the Western region storm scenario and the IEEE -39 bus system. Moreover, a novel optimal approach to restore the Western region is discussed in this chapter.

In the planning case representing summer peak conditions, the Western region load was approximately 1900 MW. Following the storm event a total of 11 lines were tripped separating the Western region from the rest of the Entergy system [39]. The lines that were tripped are shown in Table 4.1.

Table 4.1 Lines That Separated the Western Region from the System

No.	From	To
1	Fork Creek (97695)	Sam Rayburn (97704)
2	Cheek (97692)	Dayton (97632)
3	China (97714)	Sabine (97716)
4	China (97714)	Amelia (97689)
5	Hightower (97474)	Jacinto (97476)
6	Stowell (97707)	Shiloh (97725)
7	Cypress (97690)	Poco (97494)
8	Kountze (97700)	Doucette (97694)
9	Pee Dee (97512)	Rivtrin (97536)
10	Grimes (97514)	Huntsville (97484)
11	Grimes (97514)	Conroe bulk (97459)

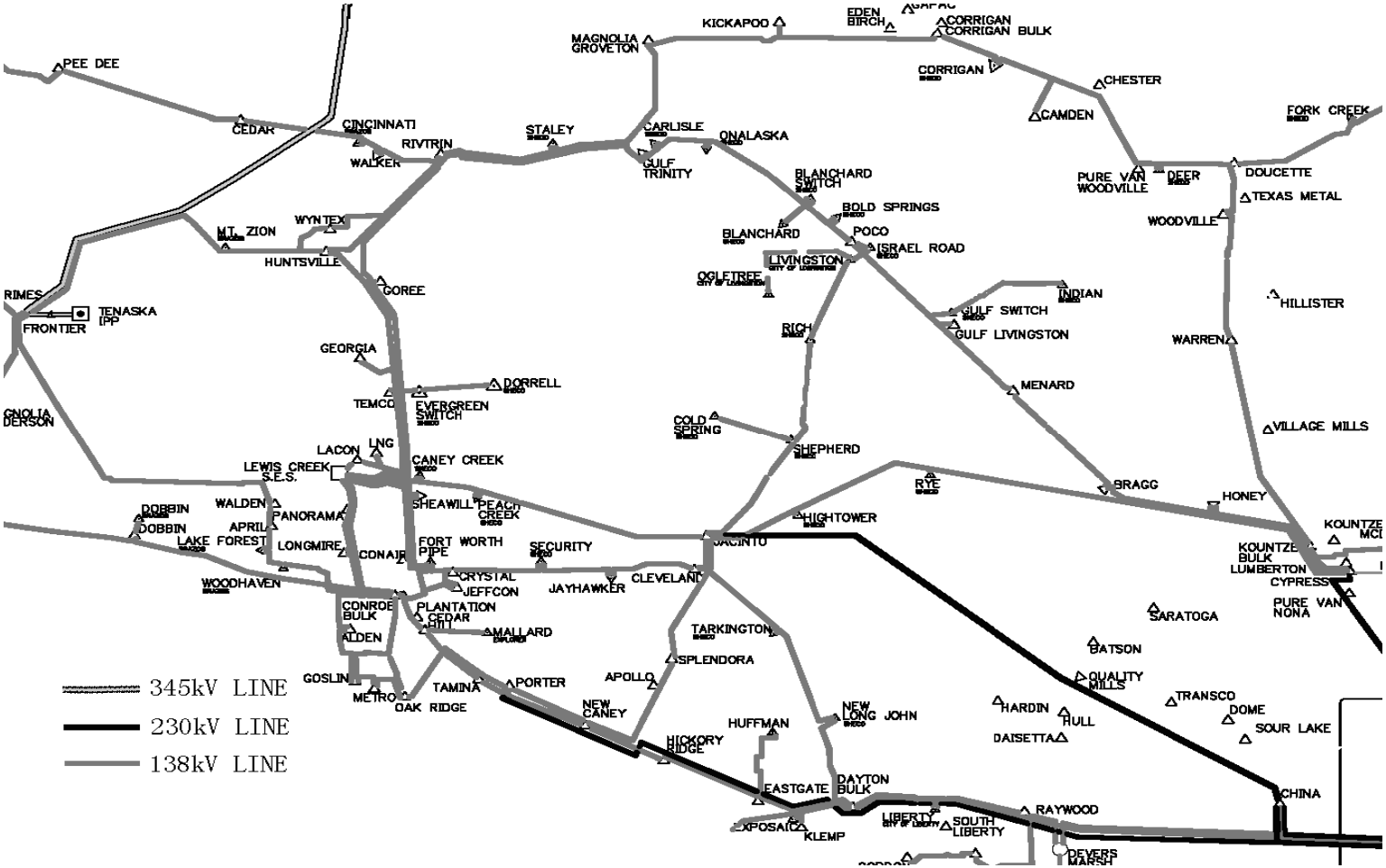

Fig. 4.1 The Western region of the Entergy system

Shortly after the disturbance event, the transmission operation center (TOC) operators started to take manual actions to switch the outaged lines back into service. The first manual action recorded in the events summary relating to the outages and the restoration activities is the restoration of the China (97714) - Amelia (97689) line at 19:04:44, approximately 8 minutes after the initial event. The restoration failed because of sustained phase B to ground fault. The first successfully restored line was Kountze (97700) – Doucett (97694) at 19:22:28, approximately 26 minutes after the initial event. The actual restoration process that was followed by the system operators is detailed in Table 4.2.

Table 4.2 System Restoration Time Log

No.	Time	Index
1	19:22:56.000	2955 KTB To DCT
2	19:24:26.000	5295 STW TO SHILOH
3	19:25:47.893	6970 POCO TO CYP
4	20:06:28.000	16515 JAC TO HIGHTOWER
5	21:01:03.000	16250 CNB TO GRI
6	21:12:25.000	6460 RVT TO PEEDEE
7	21:44:03.000	22820 CHEEK TO DAYTON
8	21:57:54.000	13260 SAB TO CHINA

From the details provided in [39], the Lewis Creek units which are the major generating units in the affected area could not meet the immediate load demand because they sustained minor damage during the event. Therefore, the entire power supply for the affected area had to be obtained from outside the affected area. Given this premise it was imperative that critical tie lines be restored

first in order to provide an outside source for black start. The application of the proposed path selection algorithm with constraint checking is detailed below.

4.3 Proposed System Restoration on Western Region of Entergy System

The steps taken by the automatic restoration path selection algorithm is as follows:

Step 1: China (97714) is chosen as the power source bus sending cranking power to the generators inside the affected area. China (97714) Substation is one of the four bulk power sources into the region. China (97714) – Jacinto (97476) and China (97714) – Porter (97567) are the only two 230 kV lines in the Western region. There is a total of 1587 MVA power injection capability into the Western region through these two lines. The transmission line China (97714) - Amelia (97689) experienced a sustained fault during the outage and is one of two 230 kV paths to the China Substation. The other line China (97714) – Sabine (97716) is the first line that the TOC operators tried to restore at 19:04:44.

The first step in the proposed approach is to provide power/voltage to the critical generator buses inside the affected area. The goal in this study is to restore voltage to the Lewis Creek (97451, 97452) generating bus/station, if the station is available and not damaged. The single line diagram is shown in Fig. 4.2.

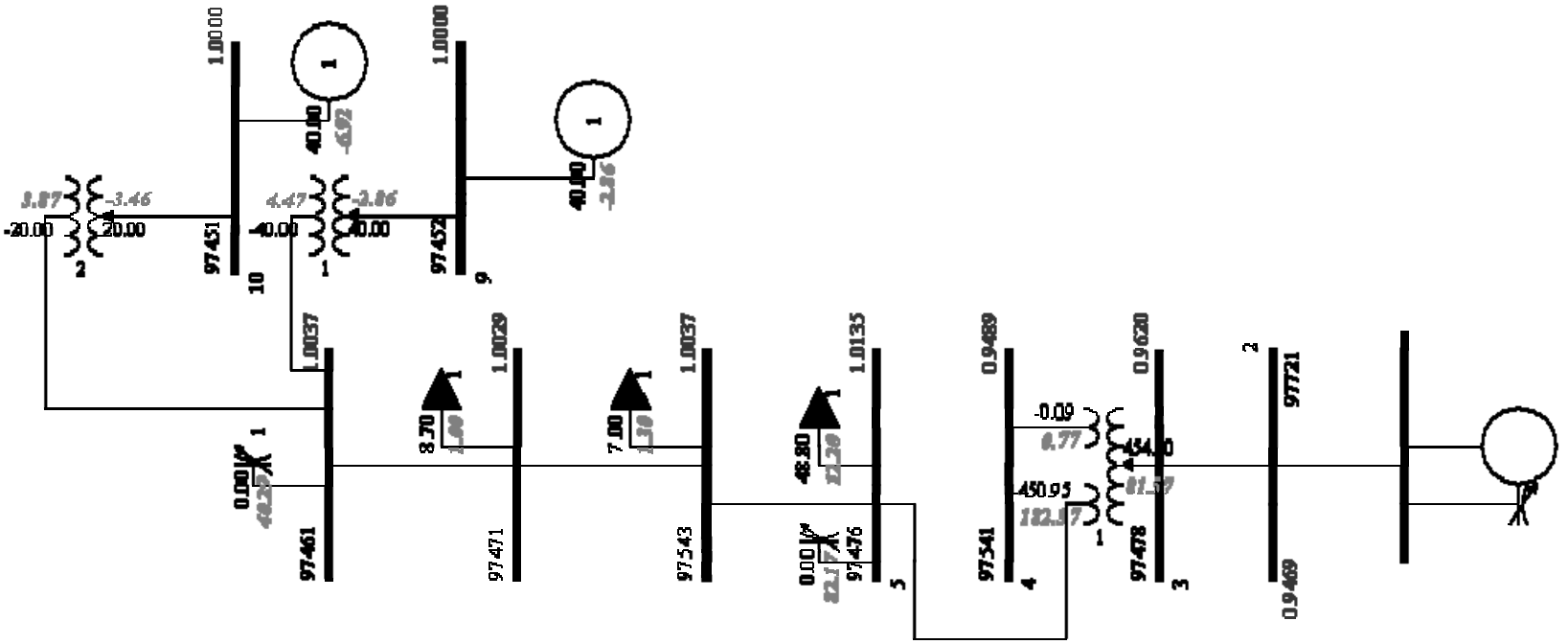

Fig. 4.2 Single line diagram connecting power source China and generator bus Lewis Creek through Jacinto

Step 2: The Woodlands area is located in the Southwest portion of the Western region, and it has a high concentration of residential and commercial loads. This area includes Conroe (97459), Alden (97544), Goslin (97468) and some other heavily loaded buses. This area is defined as Area I, and the remaining portion of the Western region as Area II. The transmission lines at the boundary between Area I and Area II are shown in Fig. 4.3 and Table 4.3.

Table 4.3 Boundary Lines Between Area I and Area II

No.	From	To
1	97475 (Cleveland)	97476 (Jacinto)
2	97461 (Lewis) Creek)	97471
3	97461 (Lewis) Creek)	97466
4	97461 (Lewis) Creek)	97458 (Conair)
5	97461 (Lewis) Creek)	97544 (Alden)
6	97567 (Porter)	97463
7	97567 (Porter)	97566
8	97459 (Conroe)	97539

N-1 dynamic contingency analysis is then simulated on both areas using TSAT software as described in Chapter 3. The results show that if Area I is restored first, 4 out of the 68 possible contingencies are insecure and all secure contingencies have an average *TSI* value of 89.85. However, if Area II is restored first, 16 out of the possible 184 contingencies are insecure and the average *TSI* for all secure contingencies is 87.98. Hence, based on the relative severity of the dynamic security assessment it is determined that load Area I should be restored before load Area II.

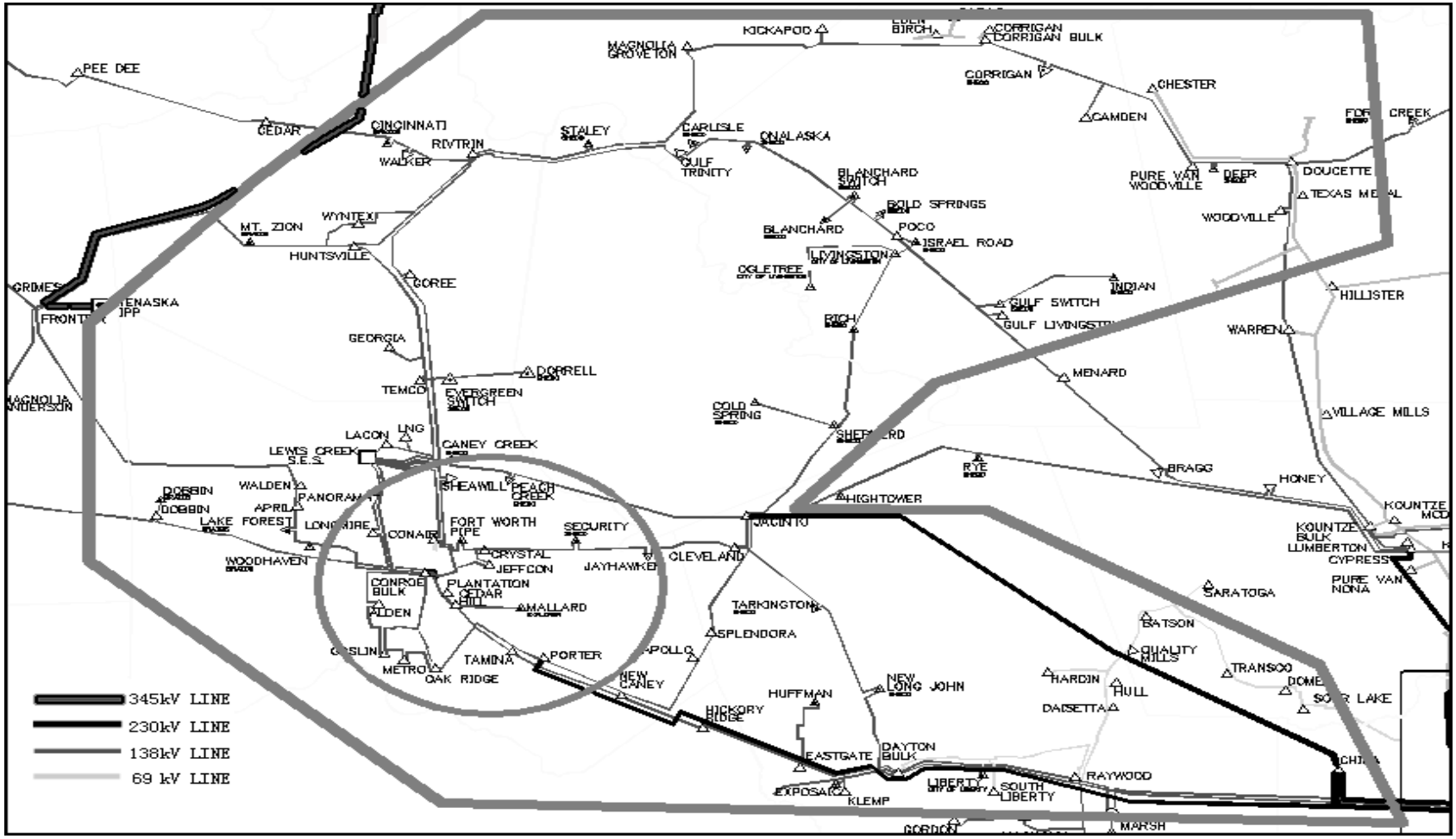

Fig. 4.3 Loads areas boundary in Western region

Once this has been ascertained the algorithm progresses systematically to determine the transmission paths to restore in order to supply the load in Area I based on the procedure described above.

Step 3: The transmission lines and loads in Area I are restored based on the RPI values of all possible transmission lines to be restored. The assumption is that the same amount of load at each end of the new radial lines will be energized. The algorithm will choose the line that is closer to the generator buses or power source buses. The system topology is quite similar to that of a tree. When one or more transmission lines are close to their transmission limit, the algorithm will force the tree to create some loops to relieve the stress on the branches. Three lines are shown below.

- 97461(Lewis Creek)- 97466- 97520 (Fort pipe)
- 97520 (Fort pipe)- 97460- 97456- 97542- 97475 (Cleveland)
- 97476 (Jacinto)-97475 (Cleveland)- 97542

In this step, both types of RPI value calculation are utilized to perform thermal constraint checking. The calculation illustration will be shown in the following section. The system one line diagram after these lines are restored is shown in Fig. 4.4.

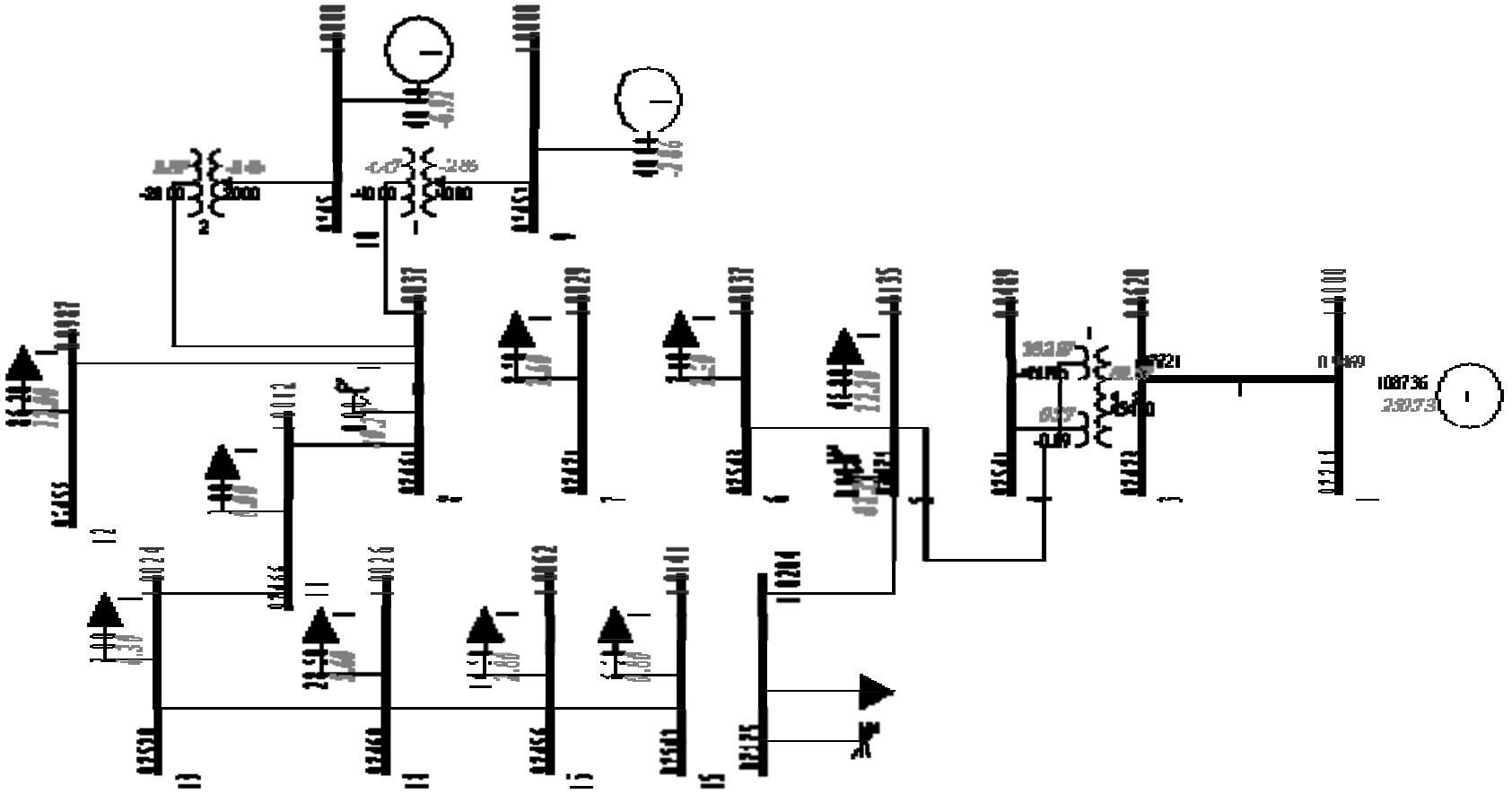

Fig. 4.4 Single line diagram in Step 3

Then, the remaining lines in Area I are restored. These include

- 97459 (Conroe)- 97465- 97511- 97566
- 97468 (Goslin)- 97455- 97463

The single line diagram with these lines restored is shown in Fig. 4.5.

Step 4: After the transmission lines supplying the load area are fully restored, *N*-1 contingency analysis is simulated on restored buses as described in Chapter 3. The maximum load level that can be supplied in order to guarantee that all *N*-1 contingencies will be secure is determined.

According to the RPI calculation, transmission lines in Area II can be picked up in sequence. After picking up the following lines, the single line diagram is shown in

- 97566 -97467 (Porter) -97567
- 97467 (Porter) -97533 -97532 (Hickory) -97627 -97754
- 97627 -97723 -97726
- 97723 -97632 (Dayton)
- 97693 (138 kV, China) -97593 -97626 (Raywood) -97724 -97632 (Dayton)
- 97626(Raywood) -97750 -97725(Shiloh)
- 97750 -97748 -97749

- 97461(Lewis) -97483 -97536 (Rivtrin)
- 97461(Lewis) -97545 -97538 -97488 -97519 -97484(Huntsvl)
- 97461 (Lewis) -97464 -97457 -97453
- 97459 (Conroe) -97539 -97470 -97469 -97454 -97514
- 97476 (Jacinto) -97479 -97495 -97489 -97494(Poco)
- 97536 (Rivtrin) -97537 -97529 -97499 -97497 -97496 -97518 -97685 -97694(Doucett)
- 97484 (Huntsvl) -97480 -97486 -97485 -97536 (Rivtrin)
- 97484(Huntsvl) -97480 -97487 -97514 (Grimes)
- 97536 (Rivtrin) -97528 -97535 -97552 -97492 -97553 -97494

The resulting load pick up curve obtained by the proposed method is then compared to the actual load pick up curve that was obtained when the Western system was restored by system operators following the storm-related outages. The plot is shown in Fig. 4.6.

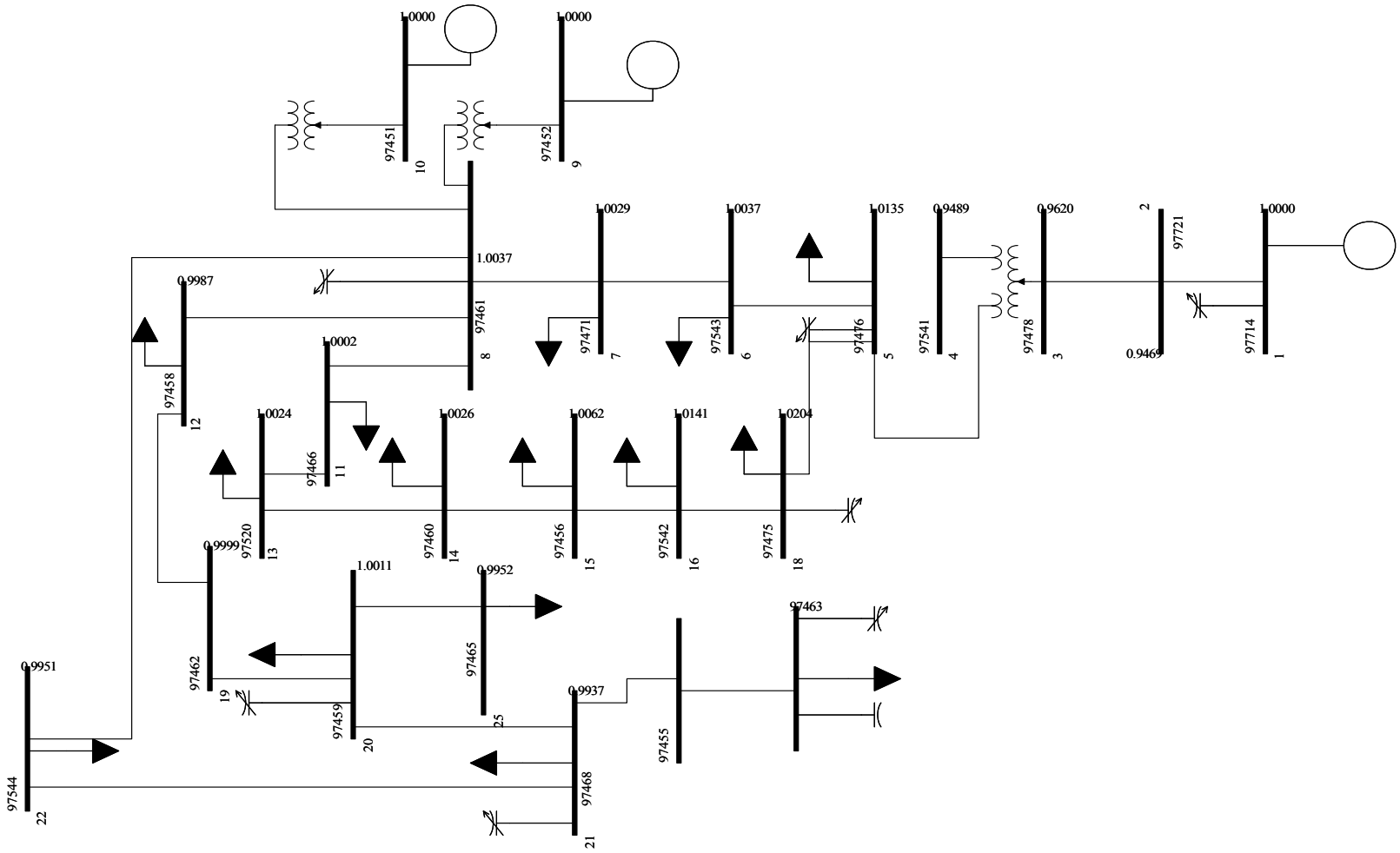

Fig. 4.5 Single line diagram with all lines restored in Area I

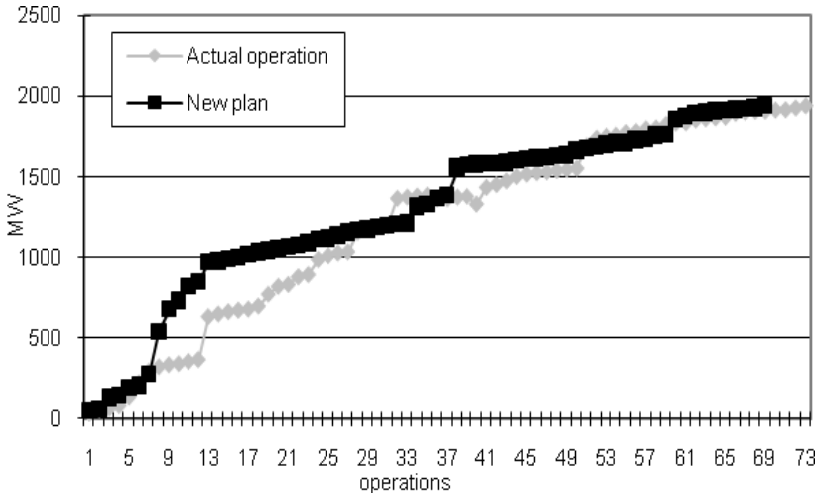

Fig. 4.6 Comparison of the load curve based on proposed method and the actual system operations on Western region of Entergy system

From the Fig. 4.6 it is observed that the new restoration path strategy generated by the program provides a more efficient approach to restore the unserved load in the system than the actual restoration operation. In addition, the transmission thermal limit and transient stability constraints are also satisfied. It is to be noted that in reality, there may be practical limitations in energizing some of the lines due to damages. Such factors were not considered in the analysis but can be easily implemented by taking the specific lines out of the list of candidate lines for potential energization.

4.4 IEEE-39 Bus System Case

In IEEE-39 bus system, which is shown in Fig. 4.7, bus 30 is assumed to be the only black start generator in the system. Two load areas are defined in Table 4.4. It should be emphasized that the system can be split into more than 2 areas if the system scale is huge. But the stability constraint checking algorithm will remain the same as described in Chapter 3.

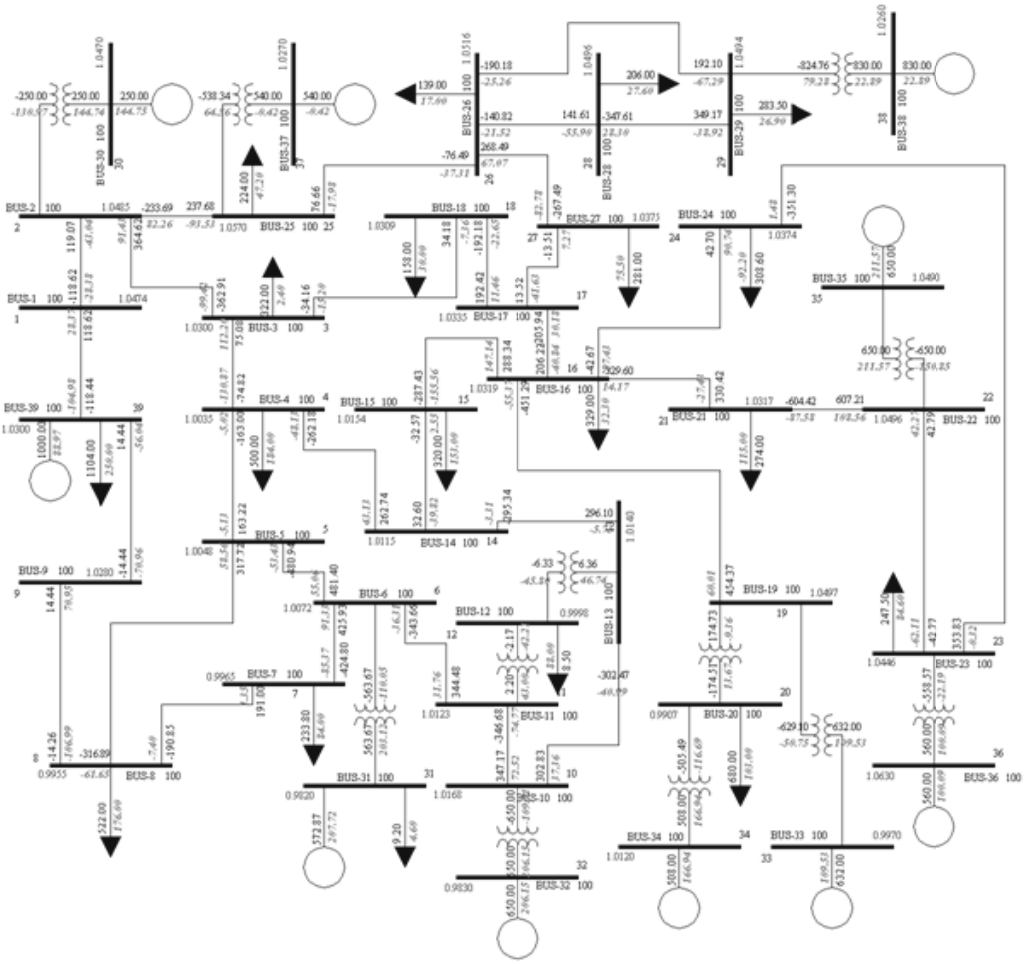

Fig. 4.7 IEEE-39 bus system

Table 4.4 Load Areas in IEEE-39 Bus System

Area	Bus Number
1	1,3,4,5,6,7,8,9,10,11,12,13,14,17,18,27,31,32,39
2	15,16,19,20,21,22,23,24,25,26,27,28,29,33,34,35,36,37,38

According to the *N-1* contingency checking result, which is shown in Table 4.5, and area determination algorithm, load Area I should be restored first. The whole system will be cranked up by PTDF-based automatic restoration path

selection algorithm.

Table 4.5 *N*-1 Contingency Checking Result

Area	Insecure *N-1* contingencies
1	0
2	4

It should be noticed that there are totally 12 buses without any generation or load on them. Based on Type I RPI algorithm, this kind of buses will have higher priority compared with generator/load bus. If both the generator bus and this kind of "empty bus" are ready to be energized, the generator bus will have the priority. The system restoration sequence and the RPI algorithm utilized are shown in Table 4.6.

Table 4.6 IEEE-39 Bus System Restoration Path

Steps	**1**	**2**	**3**	**4**	**5**	**6**	**7**	**8**	**9**	**10**
Lines	2-30	1-2	1-39	9-39	8-9	5-8	5-6	6-31	6-7	7-8
Actions	*RPI*1	*RPI*1	Crank	*RPI*1	*RPI*1	*RPI*1	*RPI*1	Crank	*RPI*1	*RPI*2
Steps	**11**	**12**	**13**	**14**	**15**	**16**	**17**	**18**	**19**	**20**
Lines	6-31	6-11	10-11	10-32	10-13	13-14	4-5	3-4	12-13	3-18
Actions	Crank	*RPI*1	*RPI*1	Crank	*RPI*1	*RPI*1	*RPI*1	*RPI*1	*RPI*1	*RPI*1
Steps	**21**	**22**	**23**	**24**	**25**	**26**	**27**	**28**	**29**	**30**
Lines	17-18	17-27	11-12	2-3	2-25	25-37	25-26	26-28	28-29	29-38
Actions	*RPI*1	*RPI*1	*RPI*2	*RPI*2	Area2	Crank	*RPI*1	*RPI*1	*RPI*1	Crank
Steps	**31**	**32**	**33**	**34**	**35**	**36**	**37**	**38**	**39**	**40**
Lines	14-15	15-16	16-19	19-33	19-20	20-34	16-21	21-22	22-35	22-23
Actions	*RPI*1	*RPI*1	*RPI*1	Crank	*RPI*1	Crank	*RPI*1	*RPI*1	Crank	*RPI*1
Steps	**41**	**42**	**43**	**44**	**45**	**46**				
Lines	16-24	23-24	16-12	4-14	26-29	26-27				
Actions	*RPI*1	*RPI*2	*RPI*2	*RPI*2	*RPI*2	*RPI*2				

4.5 Illustrations of Intermediate Steps

4.5.1 Example I: Radial Line Ranking with Type 1 RPI

After the cranking power supply is available to the generator buses in the affected area, the transmission lines and loads are restored gradually. In this case, 4 transmission lines into Area I are evaluated using the RPI_1. Assuming that 5% of the load at the end of the lines is picked up while the transmission lines are restored, the RPI calculation results are shown in Table 4.7.

Table 4.7 Type I RPI Result in Example I

Line	RPI_1 Value
97461 to 97466	7.4589
97461 to 97458	8.7566
97461 to 97544	7.5896
97476 to 97475	9.2649

Based on this ranking, the transmission line from Lewis Creek (97461) to Sheawil (97466) as shown in Fig. 4.10 is restored first. The comparison between actual power flow and the PTDF predicted power flow is shown in Fig. 4.8. The error observed is within 6%, indicating that the PTDF provides a fairly accurate estimate of system performance. The comparison of actual power flow with that predicted by PTDF after adding the other lines in Table 4.7 is shown in Fig. 4.9. From this figure, it is observed that the PTDF based power flow results are very close to those obtained by running the actual power flow. All the candidate radial lines are then evaluated using the RPI approach. The RPI values indicate the restoration priority of the lines. It is recommended that the line with the lowest RPI

value should be restored first. However, the final decision on restoring the lines could is left to the operators based on their experience and safety considerations.

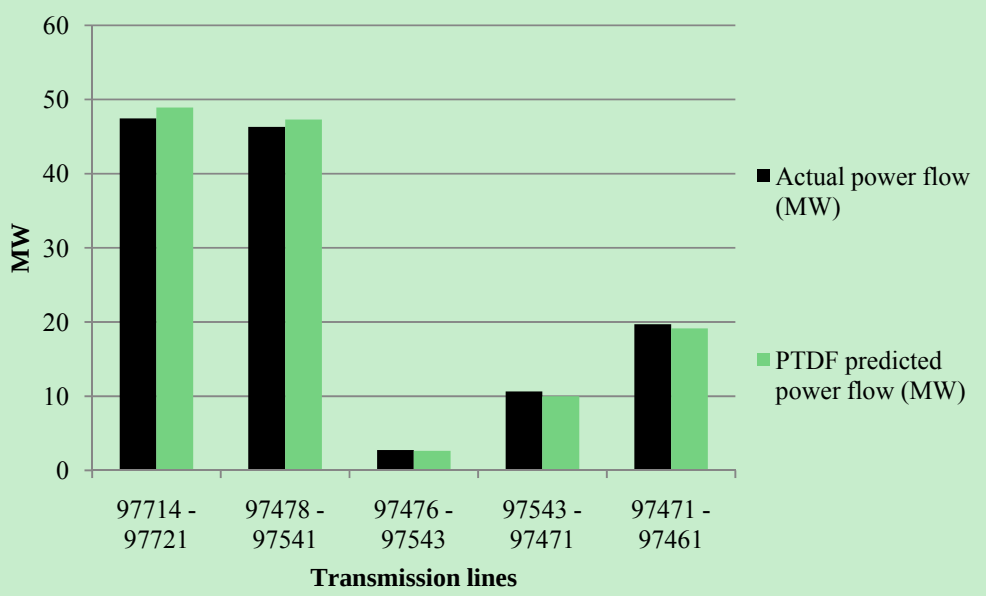

Fig. 4.8 Comparison of the actual power flow and PTDF predicted power flow

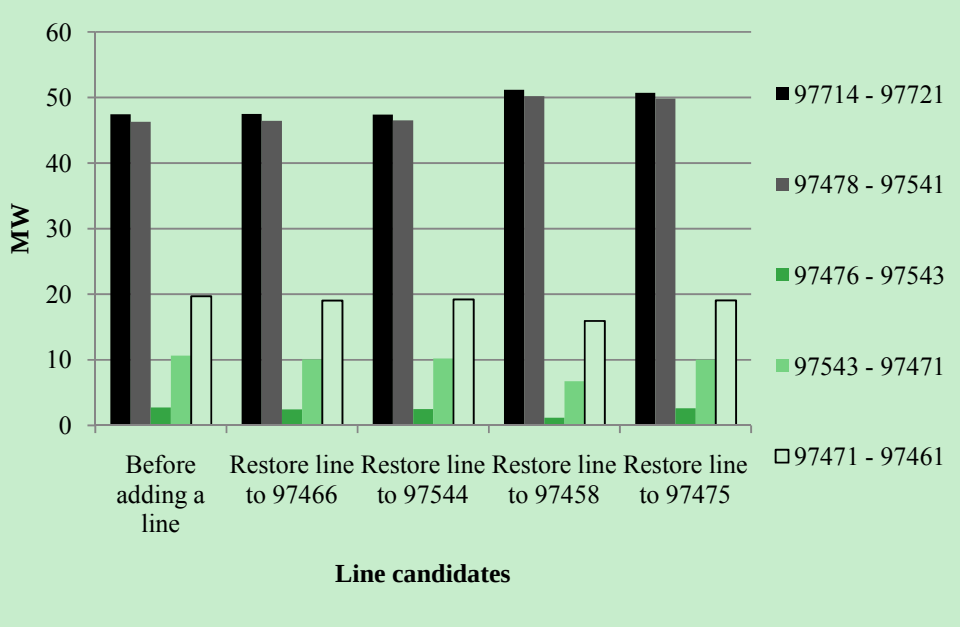

Fig. 4.9 Comparison of the actual power flow after adding lines

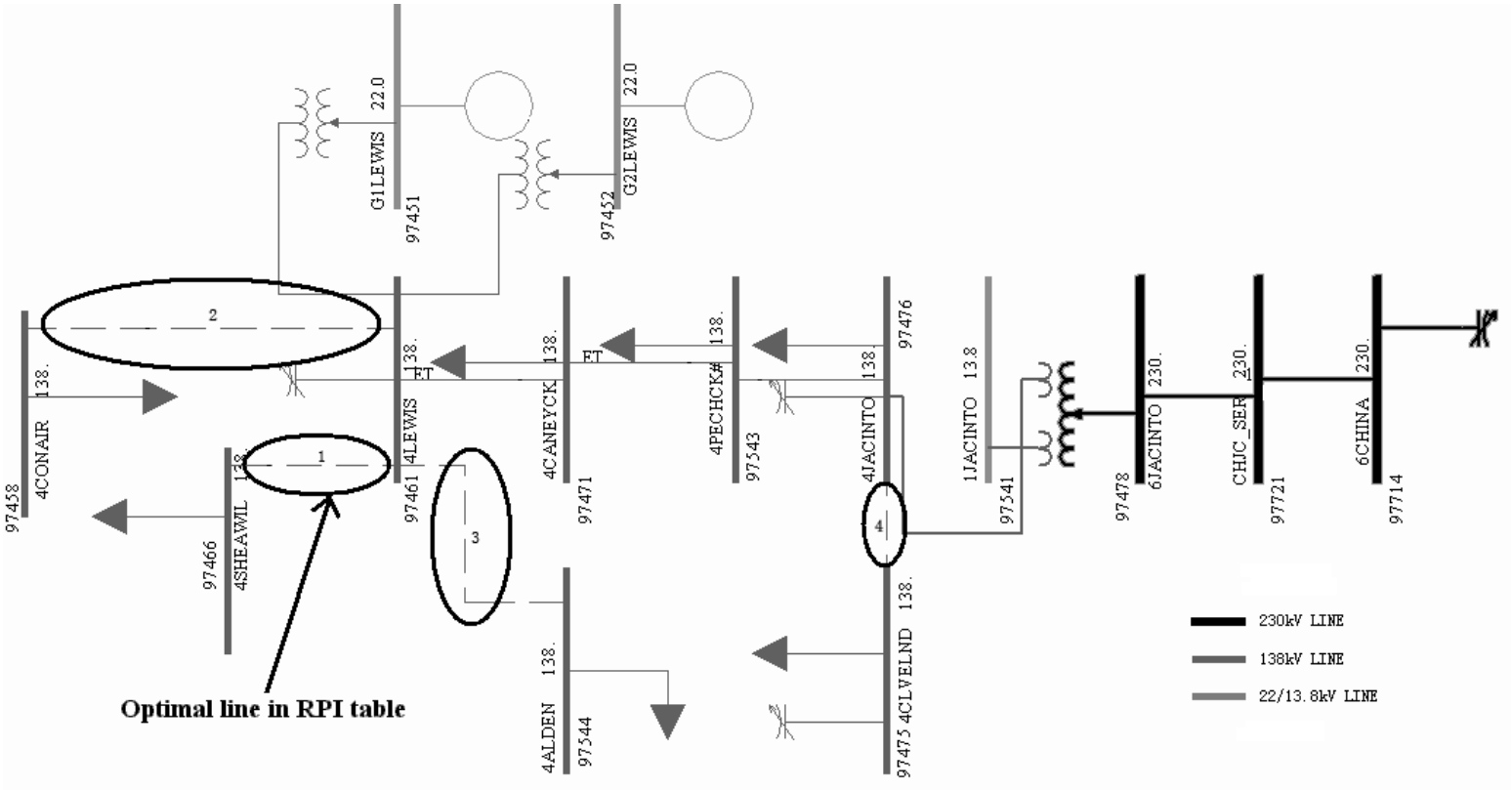

Fig. 4.10 Single line diagram showing the radial line candidates and the optimal line in RPI table after generator buses are energized, Example I

4.5.2 Example II: Loop Closure Line Ranking with Type II RPI

Since the power flow analysis indicates that the line 97476 – 97543 is within its rated limit, the algorithm developed to determine the sequence in which transmission lines are restored is then applied to determine the next transmission line to be restored. PTDFs and RPI_2 are utilized to choose the next line to be energized. Fig. 4.12 shows that when line Lewis Creek (97461) – Sheawil (97466) is close to its thermal limit, the algorithm chooses line Security (97456) – Jayhawk (97542) which is a loop closure line to be restored next. The power flow change after closing this line is shown in Table 4.8 and Fig. 4.11.

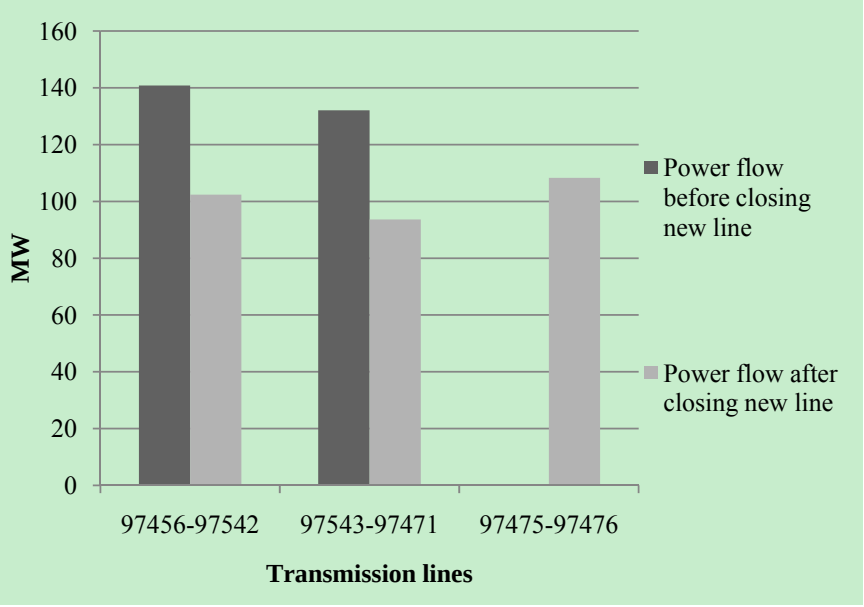

Fig. 4.11 Comparison of the power flow before and after adding loop closure line

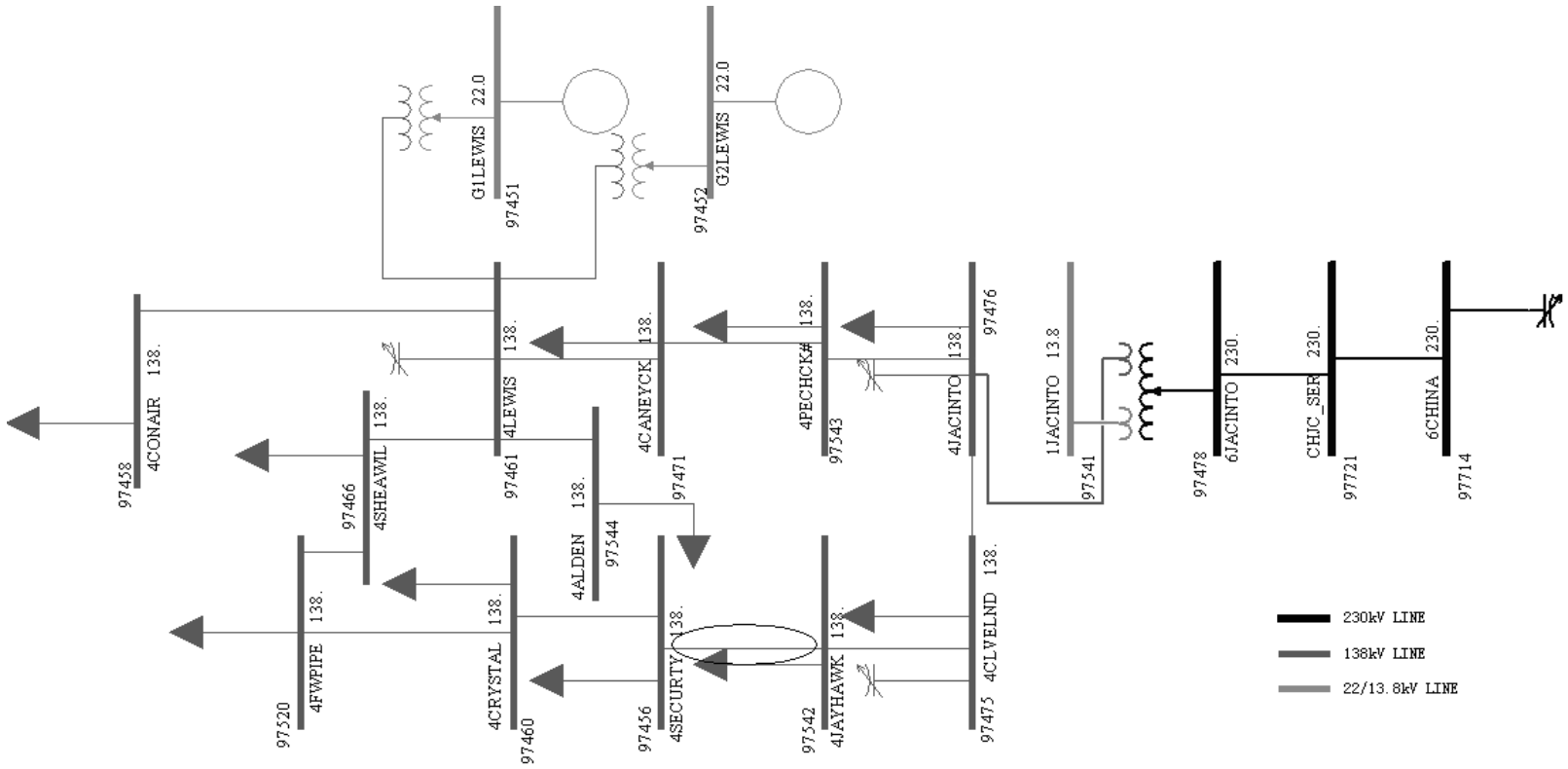

Fig. 4.12 Single line diagram showing the loop closure line Security (97456) – Jayhawk (97542) is energized due to line thermal limit on another line, Example II

Table 4.8 Type II RPI Result in Example II

No.	Line	Power Flow Before Closing New Line (MW)	Power Flow After Closing New Line (MW)
1	97456-97542	140.8	102.4
2	97543-97471	132.1	93.6
3	97475-97476	0	108.3

These results reveal that the power flow on the heavily loaded line 97456-97542 reduces from 140.8 MW to 102.4 MW (thermal limit of this line is 206 MVA), and some of the power flow is picked up by the line 97475-97476 (thermal limit of this line is 287 MVA). This relieves the stress on the heavily loaded line and fully utilizes all restored lines to speed up the system restoration.

4.5.3 Example III: Sustained Overvoltage Checking and Control

Before energizing the transmission lines selected using the RPI approach, sustained overvoltages should be evaluated to make sure no voltage violations occur. A generator terminal voltage violation example in the process of restoring line 97458-97461 is depicted in Fig. 4.13. The generator terminal voltages are shown in Fig. 4.14. Buses 97451 and 97452 are the generator buses inside the area being restored, bus 97714 is the outside black start source, which has a large generation capability.

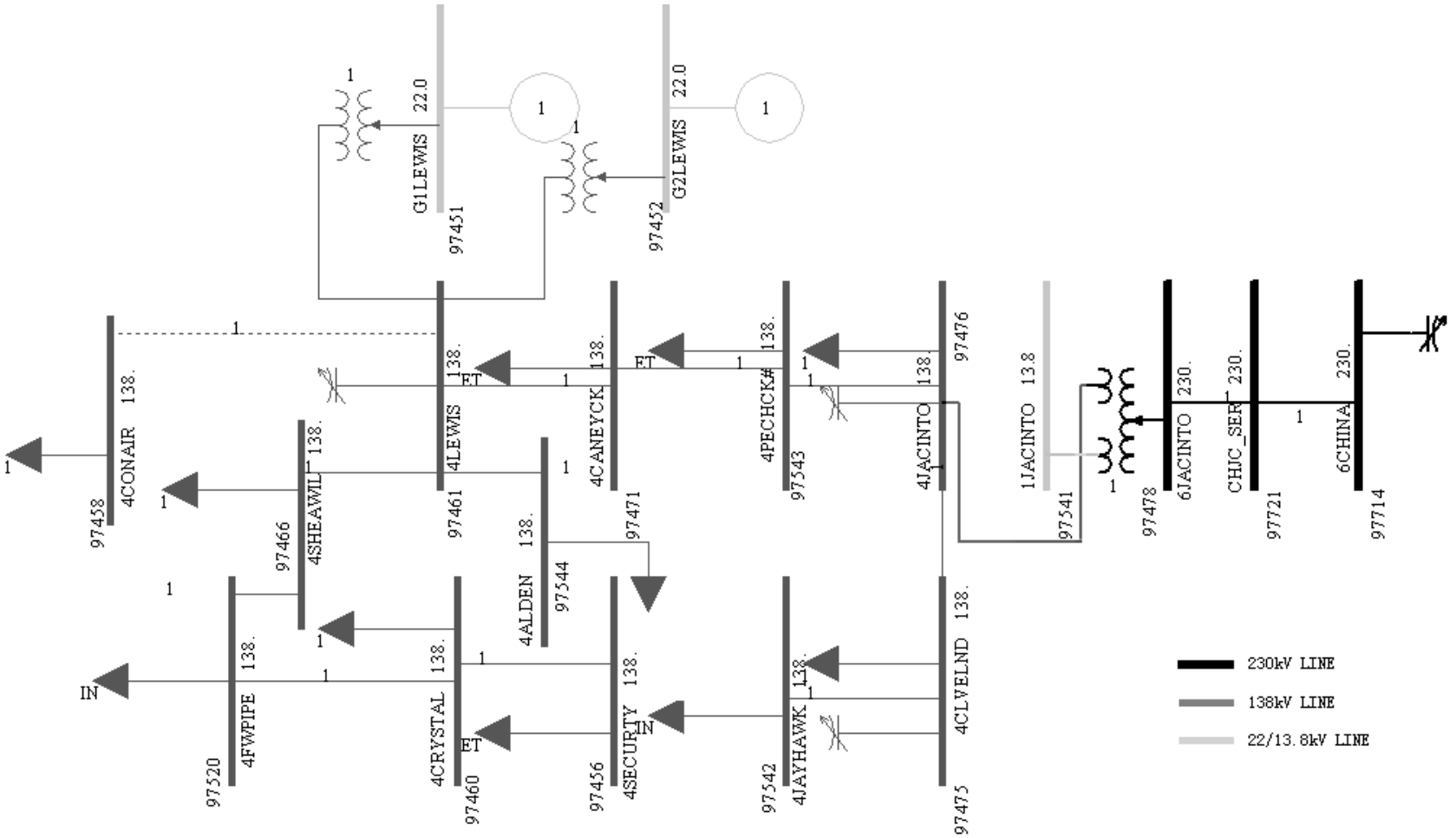

Fig. 4.13 Single line diagram showing the transmission line 97461 – 97458 (the dashed line) to be energized

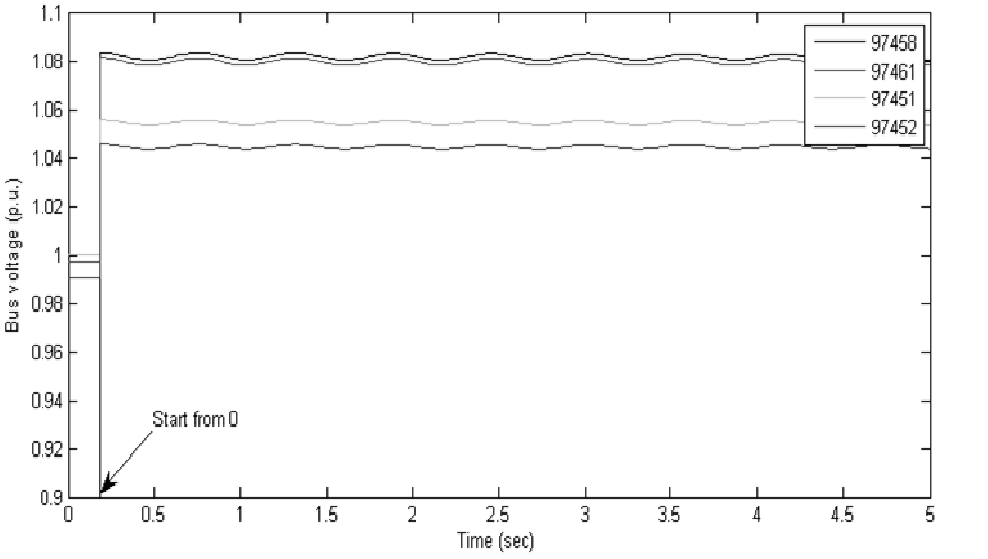

Fig. 4.14 Generator terminal voltage after restoring the line 97458-97461

If the generator terminal voltages are reduced to 0.95 p.u. before closing the line, and a shunt reactive source is also connected, the generator voltages are within the acceptable limits as shown in Fig. 4.15.

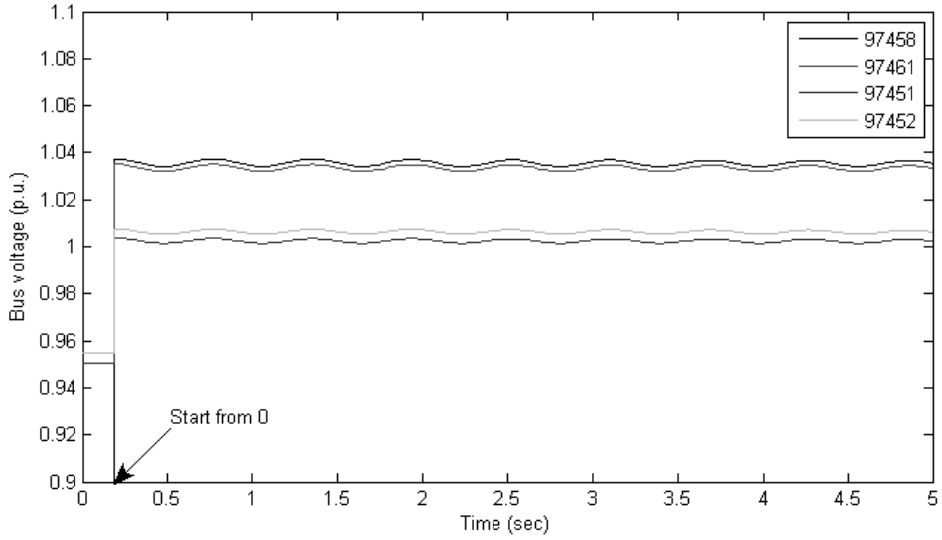

Fig. 4.15 Generator terminal voltages are reduced to 0.95 p.u. before closing the line and shunt reactive source is connected

The results show that the sustained overvoltages can be efficiently controlled by methods described in Chapter 3. It is important to note that the extent of the generator's voltage reduction is usually constrained by underexcitation of generators brought about by a number of limiting factors, including generator terminal low voltage limit, reactive ampere limit relay and minimum excitation limit relay. It may be necessary that more than one voltage control method needs to be applied in a given system.

CHAPTER 5

CONCLUSIONS AND FUTURE WORK

5.1 Conclusions

This dissertation provides a method using OBDD to split the system into suitable islands or subsystems that would facilitate restoration. The proposed strategy decomposes the spitting process into two parts: 1) determination of branches order in OBDD, 2) finding the boundary of the islands under the constraints of minimizing the generation load imbalance.

A systematic method is presented for developing an automatic restoration path selection procedure after a blackout/island occurs. The suggested approach uses the power transfer distribution factor algorithm and weighting factors to determine the optimal restoration sequence for the transmission system. This path selection procedure is performed by checking system thermal constraints, transient stability constraints and voltage constraints. The restoration path selection algorithm is intended to assist the system operator during restoration, by providing a restoration index. Two kinds of restoration performance indices (RPI) are shown. The restoration indices are effective during the restoration of the transmission system as they provide guidance to the operators on how transmission lines should be restored. The algorithm was tested on the Western region of the Entergy system. The restoration sequence for the transmission lines ensures that the thermal constraint is satisfied during the restoration and can adapt to the changing system conditions. The transient stability constraint is also checked before and after each load area is restored to make sure that the system is secure and stable.

- The OBDD-based sectionalizing method has been tested on several IEEE test systems, which include the IEEE 14, 39, 57, 118-bus systems.
- The proposed approach will sectionalize the system into suitable islands or subsystems that would facilitate parallel restoration. Then a sequential restoration would accomplish the restoration in each subsystem.
- Compared to the original restoration strategy in the Entergy system, the new restoration path strategy generated by the program provides a more efficient approach in terms of the numbers of operations to restore the unserved load in the system than the actual restoration operation.
- The transmission thermal limit, transient stability constraints and voltage constraints are guaranteed to be satisfied during the restoration process.
- Two kinds of restoration performance indices (RPI) are shown. The restoration indices are effective during the restoration of the transmission system as they provide guidance to the operators on how transmission lines should be restored.

5.2 Contributions

The contributions of this dissertation include:

1) Using OBDD method to split the system into suitable islands or subsystems that would facilitate restoration. The proposed strategy decomposes the spitting process into two parts: 1) determination of branches order in OBDD, 2) finding the boundary of the islands under the constraints of minimizing the generation-load imbalance.

2) An automatic transmission path selection method is developed and

implemented for the on-line operational environment. This computational tool that can be used to provide guidance to the operators in the operational environment so that system restoration can adapt to the changing system conditions.

3) Power transfer distribution factor method is used to evaluate all possible transmission lines that can be restored with constraint checking. This is the first time this method is used to solve the system restoration problem.

4) The proposed restoration strategy is demonstrated on a realistic power system disturbance. This demonstrates the potential to extend the proposed research approach into a practical restoration strategy and provides a feasible algorithm to design restoration plans based on given system conditions.

5.3 Future Work

In system sectionalizing, the branch order can be optimized to improve the OBDD algorithm performance. If the Boolean variables exceed 10,000, the calculation speed is not acceptable for the on-line decision. But an optimized branch ordering can improve the speed significantly.

The load buses are assumed to have same priority during the restoration in this dissertation. In actual cases, some buses may have higher priority in system restoration. A weighting factor can be introduced in the restoration path selection.

The restoration path to send the cranking power to non-black-start generators can be determined before the restoration path selection based on the generator status and availability.

Consider power market in restoration. System stability, restoration time and economy are considered as a multi-objective optimization.

Finally, some implementation and coordination issues of applying restoration strategy in realistic power systems could be considered.

REFERENCES

[1] Prabha Kundur, Power System Stability and Control, McGraw-Hill Companies Inc, 1994.

[2] X. Wang, W. Shao and V. Vittal, "Adaptive Corrective Control Strategies for Pre-Venting Power System Blackouts," the 15th Power System Computation Conference, Liege, Belgium, 2005.

[3] H. A. Dryar, R. Bailey, "Restoration of Service for Large Metropolitan System After Complete Shutdown," AIEE Trans, vol. 59, 1940.

[4] R. S. Throop, "Restoration of a 230 kV Two-Circuit Transmission Line Following the Failure of 23 Steel Towers," Proceedings of the Canadian Electrical Association Engineering and Operating Division, Quebec, Oct. 1978.

[5] E. R. Holcomb, "Emergency Restoration Plan at Dallas Power & Light Company," 33rd Annual Power Distribution Conference, 1980.

[6] K. Hisayoshi, K. Masahiko, "An Expert System Assisting Fault Analysis and Restoration of a Power System," Workshop on Expert Systems, Italy, Jan. 1987.

[7] R. J. Kafka, M. M. Adibi, "System Restoration Plan Development for a Metropolitan Electric System," IEEE Trans. on Power Apparatus and Systems, vol. 100, No. 8, pp. 3701-3711, Aug. 1981.

[8] M. M. Adibi, L. H. Fink, "Power System Restoration Planning," IEEE Trans on Power Systems, vol. 9, No. 1, pp.22-28, 1994.

[9] E. J. Simburger, F. J. Hubert, “Low Voltage Bulk Power System Restoration Simulation,” IEEE Trans. on Power Apparatus and Systems, vol. 100, No. 11 pp. 4479-4484, Nov. 1981.

[10] H. Kodama, H. Suzuki, “Interactive Restoration Control of Electric Power Systems,” Control Application for Power System Security, report 514-04, Sep. 1983.

[11] N. Kakimoto, K. Emoto, M. Hayshi, “An Application of Artificial Intelligence to Restoration of Bulk Power Systems,” Proceedings of the First Symposium on Expert Systems Applications to Power Systems, Stockholm-Helsinki, Aug. 1988.

[12] M. M. Adibi, P. Celland, L. H. Fink, H. Happ, R. J. Kafka, D. Scheurer, and F. Trefny, “Power System Restoration—A Task Force Report,” IEEE Trans. on Power Apparatus and Systems, vol. 2, No. 2, pp. 271–277, May 1987.

[13] R. D. Shultz and G. A. Mason, “Blackstart Utilization of Remote Combustion Turbines, Analytical Analysis and Field Test,” IEEE Trans. on Power Apparatus and Systems, vol. PAS-103, No. 8, pp. 2186–2191, Aug. 1984.

[14] M. M. Adibi, R. W. Alexander and B. Avramovic, "Overvoltage Control During Restoration," IEEE Trans on Power Systems, vol. 7, pp. 43-52, Nov. 1992.

[15]Q. Zhao, K. Sun, and D. Zheng et al., “A Study of System Splitting Strategies for Island Operation of Power System: A Two-Phase Method Based on OBDDs,” IEEE Trans. on Power Systems, vol. 18, No. 4, pp. 1556–1565, Nov. 2003.

[16] V. Raman and A. N. Zamfirescu, “OBDD Extraction from VHDL Gate Level Descriptions at Design Elaboration,” in Proc. Fall VHDL Int. Users Forum Workshop, pp. 30–39, 1999.

[17] F.-M. Yeh and S.-Y. Kuo, "OBDD-Based Network Reliability Calculation," Electron. Lett., vol. 33, pp. 759–760, Apr. 1997.

[18] K. Sun, D. Zheng and Q. Lu, "Searching for Feasible Splitting Strategies of Controlled System Islanding," IEE Proceedings Generation, Transmission & Distribution, vol. 153, No. 1, pp, 89-98, 2006.

[19] K. Sun, D. Zheng and Q. Lu, "Splitting Strategies for Islanding Operation of Large-Scale Power Systems Using OBDD-Based Methods," IEEE Trans. on Power Systems, vol. 18, No. 2, pp. 912–923, May 2003.

[20] C. Wang, V. Vittal, V. S. Kolluri and S. Mandal, "PTDF-Based Automatic Restoration Path Selection," IEEE Trans on Power Systems, vol. 25, No. 3, pp. 1686–1695, Aug. 2010.

[21] C. H. Papadimitriou, "Combinatorial Optimization: Algorithms and Complexity". Englewood Cliffs, NJ: Prentice-Hall, 1982.

[22] R. E. Bryant, "Graph-Based Algorithms for Boolean Function Manipulation," IEEE Trans. on Computers, vol. C-35, pp. 677–691, Aug. 1986.

[23] H.-T. Liaw, C.-S. Lin, "On the OBDD-Representation of General Boolean Functions," IEEE Trans. on Computers, vol. 41, No. 6, pp. 661–664, Jun. 1992.

[24] P. M. Anderson and M. Mirheydar, "An Adaptive Method for Setting Under-Frequency Load Shedding Relays," IEEE Trans on Power Systems, vol. 7, No. 2, pp.720–729, May 1992.

[25] H. You, V. Vittal and Z. Yang, "Self-Healing in Power Systems: An Approach Using Islanding and Rate of Frequency Decline-Based Load Shed-

ding," IEEE Trans. on Power Systems, vol. 18, No. 1, pp. 174-181, Feb. 2003.

[26] NPCC Emergency Operation Criteria. [Online]. Available: http://www.npcc.org/viewDoc.aspx?name=PRC-006-NPCC-01_082709.pdf&cat=openProcess

[27] Powertech Labs Inc., DSATools, Surrey, British Columbia, Canada.

[28] Jørn Lind-Nielsen's BuDDy Package. [Online]. Available: http://sourceforge.net/projects/buddy/develop

[29] R. D. Shultz and G. A. Mason, "Blackstart Utilization of Remote Combustion Turbines, Analytical Analysis and Field Test," IEEE Trans. on Power Apparatus and Systems, vol. PAS-103, No. 8, pp. 2186–2191, Aug. 1984.

[30] M. M. Adibi, D. P. Milanicz, and T. L. Volkmann, "Remote Cranking of Steam Electric Station," IEEE Trans. on Power Systems, vol. 11, No. 3, pp. 1613–1618, Aug. 1996.

[31] C. C. Liu, S. J. Lee, and S. S. Venkata, "An Expert System Operational Aid for Restoration and Loss Reduction of Distribution Systems," IEEE Trans. on Power Systems, vol. 3, No. 2, pp. 619–626, May 1988.

[32] Y. Fukuyama, H. Endo, and Y. Nakanishi, "A Hybrid System for Service Restoration Using Expert System and Genetic Algorithm," Intelligent Systems Applications Power Systems, Jan. 1996.

[33] M.M. Adibi, J.N. Borkoski, L.R. Kafka, "Frequency Response of Prime Movers During Restoration," IEEE Trans. on Power Systems, vol. 14, No. 2, pp. 751–756, May 1999.

[34] A. J. Wood, and B. F. Wollenberg, Power Generation, Operation, and Control, 2nd ed. New York: Wiley-Interscience, 1984.

[35] G. T. Heydt, Computer Analysis Methods for Power Systems. Stars in a Circle Publications, 1996.

[36] R. Pérez-Guerrero, G. T. Heydt, "Optimal Restoration of Distribution Systems Using Dynamic Programming," IEEE Trans. on Power Delivery, vol. 23, No. 3, pp. 1589–1596, Jul. 2008.

[37] M. Zima, G. Andersson, "On Security Criteria in Power Systems Operation," IEEE Power Engineering Society General Meeting, vol. 3 pp.3089-3093 Jun 2005.

[38] Powertech Labs Inc., DSA Tools model manual, Version 7.1.

[39] V.S. Kolluri, S. Mandal, "Simulation and Analysis of a Major Disturbance in Entergy System That Resulted in Voltage Collapse," IEEE Power Engineering Society General Meeting, pp. 6, 2003.